



Article

# Examining the Transcriptomic and Biochemical Signatures of *Bacillus subtilis* Strains: Impacts on Plant Growth and Abiotic Stress Tolerance

Peter E. Chang, Yun-Hsiang Wu, Ciao-Yun Tai, I-Hung Lin, Wen-Der Wang , Tong-Seung Tseng \*  
and Huey-wen Chuang \*

Department of Agricultural Biotechnology, National Chiayi University, Chiayi 600355, Taiwan; s1082391@mail.ncyu.edu.tw (C.-Y.T.); s1100111@mail.ncyu.edu.tw (I.-H.L.)

\* Correspondence: tsengts@mail.ncyu.edu.tw (T.-S.T.); hwchuang@mail.ncyu.edu.tw (H.-w.C.)

**Abstract:** Rhizobacteria from various ecological niches display variations in physiological characteristics. This study investigates the transcriptome profiling of two *Bacillus subtilis* strains, BsCP1 and BsPG1, each isolated from distinct environments. Gene expression linked to the synthesis of seven types of antibiotic compounds was detected in both BsCP1 and BsPG1 cultures. Among these, the genes associated with plipastatin synthesis were predominantly expressed in both bacterial strains. However, genes responsible for the synthesis of polyketide, subtilosin, and surfactin showed distinct transcriptional patterns. Additionally, genes involved in producing exopolysaccharides (EPS) showed higher expression levels in BsPG1 than in BsCP1. Consistently with this, a greater quantity of EPS was found in the BsPG1 culture compared to BsCP1. Both bacterial strains exhibited similar effects on *Arabidopsis* seedlings, promoting root branching and increasing seedling fresh weight. However, BsPG1 was a more potent enhancer of drought, heat, and copper stress tolerance than BsCP1. Treatment with BsPG1 had a greater impact on improving survival rates, increasing starch accumulation, and stabilizing chlorophyll content during the post-stress stage. qPCR analysis was used to measure transcriptional changes in *Arabidopsis* seedlings in response to BsCP1 and BsPG1 treatment. The results show that both bacterial strains had a similar impact on the expression of genes involved in the salicylic acid (SA) and jasmonic acid (JA) signaling pathways. Likewise, genes associated with stress response, root development, and disease resistance showed comparable responses to both bacterial strains. However, treatment with BsCP1 and BsPG1 induced distinct activation of genes associated with the ABA signaling pathway. The results of this study demonstrate that bacterial strains from different ecological environments have varying abilities to produce beneficial metabolites for plant growth. Apart from the SA and JA signaling pathways, ABA signaling triggered by PGPR bacterial strains could play a crucial role in building an effective resistance to various abiotic stresses in the plants they colonize.

**Keywords:** transcription profiling; exopolysaccharide; ABA signaling; drought stress tolerance; heat stress tolerance; copper stress tolerance



**Citation:** Chang, P.E.; Wu, Y.-H.; Tai, C.-Y.; Lin, I.-H.; Wang, W.-D.; Tseng, T.-S.; Chuang, H.-w. Examining the Transcriptomic and Biochemical Signatures of *Bacillus subtilis* Strains: Impacts on Plant Growth and Abiotic Stress Tolerance. *Int. J. Mol. Sci.* **2023**, *24*, 13720. <https://doi.org/10.3390/ijms241813720>

Academic Editor: Jen-Tsung Chen

Received: 10 August 2023

Revised: 3 September 2023

Accepted: 4 September 2023

Published: 6 September 2023



**Copyright:** © 2023 by the authors. Licensee MDPI, Basel, Switzerland. This article is an open access article distributed under the terms and conditions of the Creative Commons Attribution (CC BY) license (<https://creativecommons.org/licenses/by/4.0/>).

## 1. Introduction

The microorganisms known as plant growth-promoting rhizobacteria (PGPR) are a diverse set of microorganisms that colonize the rhizosphere and stimulate plant growth via various mechanisms. Rhizobacteria produce diverse metabolites to function as communication signals within the microbial ecosystem. This may provide them an advantage in the competition for resources and habitats against other organisms. Certain metabolites from PGPR strains can have a direct effect on plant development. For example, the production of indole-3-acetic acid (IAA), a prevalent form of the phytohormone auxin, is commonly found among bacteria. IAA can serve a role in facilitating communication between cells within and among microbial communities, as well as in interactions between

plants and microbes [1]. In plant cells, the regulatory role of auxin is evident throughout all stages of the plant life cycle. In particular, the essential role of auxin in lateral root development has been widely recognized [2]. IAA, produced by PGPR strains, positively influences root branching and vegetative growth [3]. Microbial bacillibactin, a catechol type siderophore, not only works as a biocontrol agent, but also promotes plant growth by improving iron absorption [4]. However, the metabolites produced by PGPR strains can also boost plant growth through indirect processes. For example, applying PGPR that produce 1-aminocyclopropane-1-carboxylate (ACC) deaminase promotes plant growth by mitigating the harmful effects of ethylene production under stressful conditions [5]. Rhizobacteria can produce various types of volatile compounds (VOCs) that not only facilitate interactions between microorganisms but also have the ability to modulate plant growth and stress tolerance by altering phytohormone signaling pathways [6–9]. Surfactin, a cyclic lipopeptide, plays multiple roles in microorganisms, including promoting biofilm formation, facilitating cell motility, and engaging in competition with other microorganisms [10]. In plant cells, surfactin can trigger early events that are associated with the induction of defense responses, such as extracellular alkalization, the accumulation of reactive oxygen species (ROS), and the activation of defense-related enzymes like lipoxygenase [11]. Exopolysaccharides (EPSs) are the main components for biofilm structure formation [12]. EPSs can act as chelating agents, limiting the uptake of heavy metals in plant roots and enhancing chlorophyll and osmolyte concentrations, thus mitigating cellular damage under drought stress [13,14].

The metabolites produced by PGPR can promote plant growth by altering multiple plant signaling pathways that are involved in the regulation of adaptive responses under stressful conditions [15]. Plants encounter various abiotic stresses that impose negative effects on their growth and productivity. During stages of water shortage, the closing of stomata is a strategy to prevent excessive water loss. However, this process also inhibits CO<sub>2</sub> absorption in the leaves, leading to a reduction in photosynthesis. This in turn results in an accumulation of ROS, which could be detrimental to the photosystem and instigate chlorophyll degradation [16]. Heat stress disrupts protein function and results in metabolic irregularities. As a consequence, there is an increase in oxidative stress, which can have harmful impacts on plant growth [17]. Heavy metals have the potential to interrupt cellular activities by replacing essential metals and inducing protein misfolding and aggregation. These events can impact protein stability and decrease cell viability. Moreover, certain redox-reactive heavy metals, such as iron and copper, can produce ROS molecules through the Fenton reaction [18]. The build-up of ROS is a common factor contributing to cellular damage under various abiotic stresses. Consequently, the fitness of plants in stressful environments heavily relies on their antioxidant defense system, which consists of antioxidant enzymes and secondary metabolites possessing ROS scavenging activity [19]. Apart from ROS signaling, the signaling pathways of phytohormones play significant roles in the regulation of plant response to abiotic stress. For example, the expression of *9-cis-epoxycarotenoid dioxygenase 3 (NCED3)*, which encodes a rate-limiting enzyme for the synthesis of abscisic acid (ABA), is induced to higher levels in response to a water deficit signal. [20]. The synthesis of ABA prompts the activity of respiratory burst oxidase homologues (RBOHs), leading to the production of ROS. This results in the closure of stomata and the prevention of water loss [21]. Systemic immunity, triggered by microbe–plant interaction, encompasses both systemic acquired resistance (SAR) and induced systemic resistance (ISR). SAR is a long-lasting form of resistance against pathogens that requires salicylic acid (SA) as a signal molecule [22]. ISR is activated by microorganisms residing in the rhizosphere, with jasmonic acid (JA) acting as a signal molecule to activate this induced resistance [22]. In addition to their roles in induced disease resistance, recent studies also indicate an important role of SA and JA signaling in the regulation of abiotic stress tolerance through mediating antioxidant activity and osmolyte accumulation [23,24]. The antioxidant defense system has been reported to be activated by SA, which helps improve the function of photosystems under heat stress [25]. The application of SA can

promote the accumulation of proline, which helps to counteract the osmotic stress generated in high-temperature environments and enhance heat stress tolerance [26]. Similarly, it has been reported that exogenous JA can activate the antioxidant defense system, modify osmotic adjustment, and improve heat stress tolerance [27].

The metabolites of PGPR strains can positively regulate plant growth by modulating phytohormone signaling pathways linked to plant development. Research has indicated that microbial VOCs can induce systemic resistance against both abiotic and biotic stress by altering the SA and ABA signaling pathways [6–8]. A primary constituent of VOCs produced by rhizobacteria, 2,3-Butanediol (2,3-BD), has been shown to enhance disease resistance and activate the auxin signal in plants when applied [9,28]. Surfactin triggers cellular pathways linked to SA and JA signaling to induce disease resistance in wheat against pathogen attacks [29]. Rhizobacteria that produce polyamines, components of biofilms, have been found to activate the ABA signaling pathway, thereby enhancing drought stress tolerance in plants [30,31]. The use of the *Bradyrhizobium japonicum* strain has been reported to activate JA signaling, priming *Arabidopsis* for improved salt stress tolerance [32]. A *B. cereus* strain that is capable of producing VOCs and serine proteases has been found to confer tolerance to multiple abiotic stresses in plants. This tolerance is achieved through the modulation of the auxin, ABA, and JA signaling pathways, as well as the stimulation of antioxidant enzymes and secondary metabolites that have ROS scavenging capabilities [33].

Studies have shown that root exudates secreted from different plant species are able to attract various microorganisms to colonize their rhizosphere [34]. Furthermore, rhizobacteria from different environments have different abilities to produce bioactive metabolites that affect plant growth [35]. In this study, two *B. subtilis* strains isolated from different sources displayed distinct transcription profiles for genes related to the synthesis of antibiotic compounds, the siderophore metabolite bacillibactin, and the biofilm constituent EPS. These two bacterial strains showed similar effects in promoting root and shoot growth but differed in their effectiveness to induce plant tolerance against drought, heat, and copper stress. Both strains activated genes associated with the SA and JA signaling pathways and abiotic and biotic stress responses, as well as root growth and development. However, the expression of genes implicated in the ABA signaling pathway responded differently to treatment with BsCP1 and BsPG1.

## 2. Results

### 2.1. Molecular Identification of BsCP1 and BsPG1

The DNA sequences of the 16S ribosomal DNA fragments obtained from BsCP1 and BsPG1 were analyzed, revealing a phylogenetic relationship with different *Bacillus subtilis* strains (Figure 1). For further verification of these two bacterial strains, PCR analysis was performed to detect gene fragments involved in the synthesis of bacillibactin, including *DbhF*, *DbhB*, and *DbhE* [36], as well as *sfp*, which is responsible for the synthesis of surfactin [37], in the genomes of BsCP1 and BsPG1 (Figure 1B). The DNA sequences of these PCR fragments were subsequently analyzed using the BLAST program, showing 99% to 100% identity to sequences from different *B. subtilis* strains (Figure 1C).

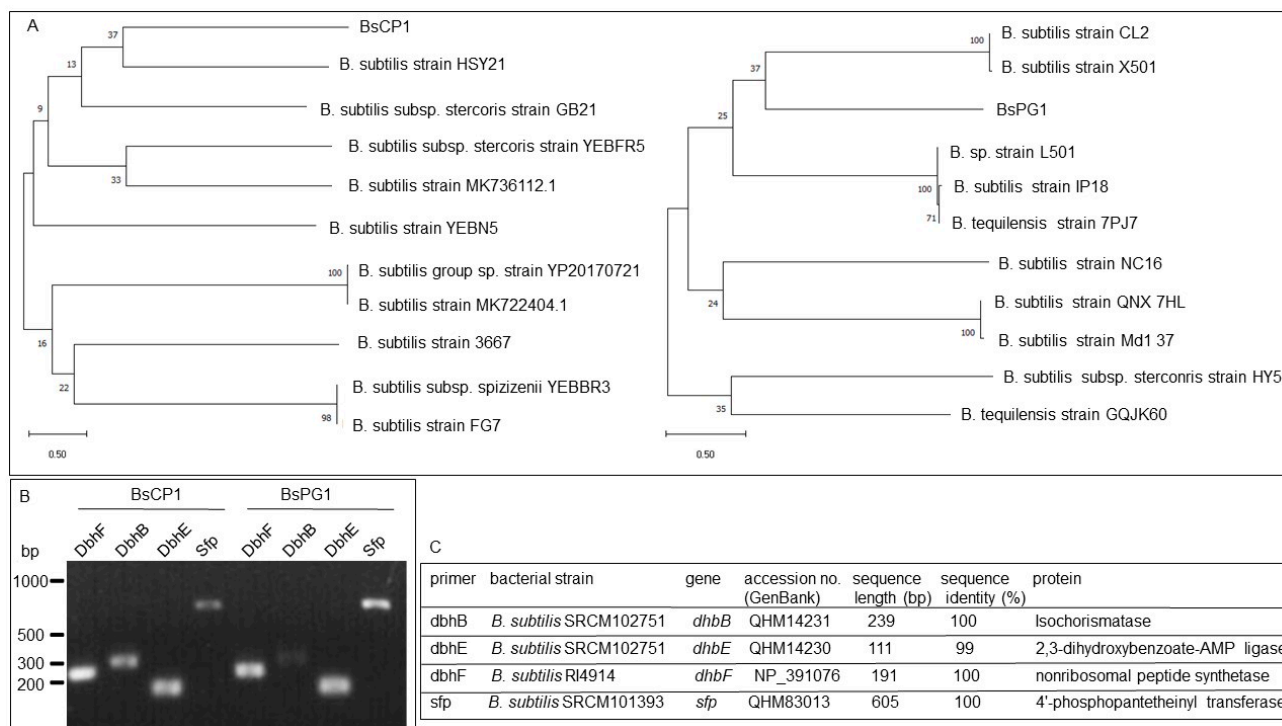


**Figure 1.** Characterization of BsCP1 and BsPG1. The 16S rDNA sequences from various *B. subtilis* strains were used for construction of a phylogenetic tree for BsCP1 (left) and BsPG1 (right) (A). Electrophoresis of PCR products generated from the genomic DNA of BsCP1 and BsPG1 (B). BLAST results for the gene segments derived from PCR amplification (C).

## 2.2. Transcriptome Analysis of BsCP1 and BsPG1

BsCP1 and BsPG1 are two *B. subtilis* strains isolated from different environments. To predict bioactive metabolites produced by these two bacterial strains, RNA-seq analyses were employed to investigate their transcriptome profiles during both the log and stationary phases of culture. A total of 4458 genes from the BsCP1 culture and 4308 genes from the BsPG1 culture were analyzed. Of these, 60.8% and 76.9% of genes were up-regulated more than two-fold during the stationary phase in comparison to their expression levels in the log phase in the BsCP1 and BsPG1 cultures, respectively. For further analysis, gene transcripts involved in the synthesis of bioactive compounds linked to plant growth-promoting traits were selected. These genes participated in the production of seven types of antibiotics, biofilm components (e.g., EPS and spermidine), VOCs like terpenoids and 2,3-BD, the phytohormone IAA, the siderophore bacillibactin, serine proteases, and phosphate-solubilizing (PS) phosphatases. As a result, a total of 54 and 72 genes were identified in BsCP1 and BsPG1, respectively (Table 1). Their distribution within each gene group is shown in Figure 2A. Genes associated with the synthesis of various antibiotic compounds represented the largest group among genes correlated to plant growth-promoting traits in both bacterial strains, BsCP1 and BsPG1, accounting for 45% and 43%, respectively. Genes linked to the synthesis of IAA constituted the second largest group in both strains, representing 13%. Both bacterial strains contained genes responsible for producing seven antibiotic metabolites, including plipastatin (also known as fengycin), bacilysin, kanosamine, polyketide, phenazine, subtilosin, and surfactin (Figure 2B). Among these, in both BsCP1 and BsPG1, three major gene groups were found to be involved in the synthesis of plipastatin, subtilosin, and surfactin. However, the number of genes responsible for the synthesis of polyketide displayed a noticeable difference between BsCP1 and BsPG1: they constituted 13% in BsCP1 and 26% in BsPG1.

**Table 1.** Genes related to plant growth-promoting traits.

Acc. No.	Gene	Log <sub>2</sub> [FC]	Acc. No.	Gene	Log <sub>2</sub> [FC]
<b>BsCP1</b>			<b>BsPG1</b>		
Plipastatin					
WP_089172562	<i>PpsC</i>	3.2	WP_086343904	<i>PpsC</i>	3.5
WP_032723105	<i>PpsB</i>	3.0	WP_129092450	<i>PpsB</i>	3.1
WP_160214989	<i>PpsA</i>	4.2	WP_101169517	<i>PpsA</i>	2.9
WP_129092448	<i>PpsD</i>	3.8	WP_080262617	<i>PpsE</i>	4.2
WP_186453377	<i>PpsD</i>	2.4	WP_128737913	<i>PpsD</i>	3.5
			WP_129092448	<i>PpsD</i>	4.5
Bacilysin					
WP_003244300	<i>BacB</i>	1.8	WP_003244300	<i>BacB</i>	2.2
WP_032722711	<i>BacD</i>	1.9	WP_124059367	<i>BacD</i>	1.2
Kanosamine					
WP_032721285	<i>NtdB</i>	0.5	WP_101169444	<i>NtdA</i>	0.7
AFQ56969	<i>NtdC</i>	7.9	WP_024572383	<i>NtdB</i>	0.5
WP_019712355	<i>NtdA</i>	0.7			
Polyketide					
WP_080287605	<i>PksL</i>	0.9	WP_185184354	<i>PksL</i>	3.5
WP_003231805	<i>PksG</i>	2.0	WP_024573082	<i>PksG</i>	3.2
WP_124048390	<i>PksF</i>	0.1	WP_173614094	<i>PksF</i>	3.0
			WP_124059875	<i>PksL</i>	2.9
			TDY57959	<i>PksN</i>	2.8
			AGZ20286	<i>PksD</i>	3.2
			WP_167559687	<i>PksJ</i>	3.1
			AGZ20287	<i>PksD</i>	3.0
Phenazine					
WP_032723009	<i>PhzF</i>	1.5	WP_069837383	<i>PhzF</i>	1.9
Subtilosin					
WP_019712818	<i>AlbD</i>	−0.1	WP_123374486	<i>AlbD</i>	0.7
WP_003222006	<i>AlbB</i>	2.3	QHF59890	<i>Syn. Pro</i>	0.8
WP_032722691	<i>AlbA</i>	1.3	WP_003222006	<i>AlbB</i>	0.4
WP_003222002	<i>BesA</i>	6.1	WP_123374484	<i>AlbA</i>	−1.6
WP_015250988	<i>AlbG</i>	1.2	WP_003222002	<i>Sub. A</i>	−3.0
			WP_021480840	<i>AlbG</i>	0.8
Surfactin					
WP_144481589	<i>SrfAA</i>	−4.1	WP_137200567	<i>SrfAA</i>	2.3
WP_029726578	<i>SrfAD</i>	−2.6	WP_185184456	<i>SrfAD</i>	3.2
WP_032722905	<i>SrfAC</i>	−4.2	WP_185184457	<i>SrfAC</i>	1.4
WP_160215003	<i>SrfAA</i>	−2.7	WP_167559147	<i>SrfAA</i>	1.3
WP_015715234	<i>Sfp</i>	0.0	WP_003234549	<i>sfp</i>	3.1
			WP_129092244	<i>SrfAB</i>	1.0
Phosphatase					
WP_003245272	<i>PhoH</i>	2.6	WP_080009778	<i>PhoA</i>	5.4
WP_010886458	<i>PhoA</i>	2.1	WP_101169869	<i>PhoD</i>	6.7
WP_032722881	<i>PhoD</i>	0.8	WP_076458498	<i>PhoB</i>	5.6
WP_080287651	<i>PhoB</i>	1.6	WP_014476350	<i>PhoE</i>	3.1
WP_003233157	<i>PhoE</i>	1.0	WP_014477373	<i>PhoH</i>	0.7
WP_014477373	<i>PhoH</i>	0.6	WP_129092478	<i>phytase</i>	6.2
WP_003230820	<i>phytase</i>	6.6			

Table 1. Cont.

Acc. No.	Gene	Log <sub>2</sub> [FC]	Acc. No.	Gene	Log <sub>2</sub> [FC]
<b>BsCP1</b>			<b>BsPG1</b>		
<b>IAA</b>					
WP_032722039	<i>TrpC</i>	0.5	WP_003230601	<i>TrpC</i>	3.1
WP_003245959	<i>TrpD</i>	0.7	WP_134981823	<i>TrpD</i>	3.7
WP_032722038	<i>TrpB</i>	1.4	WP_128737986	<i>TrpB</i>	4.2
WP_032722040	<i>TrpE</i>	−0.3	WP_032722040	<i>TrpE</i>	3.7
WP_003233236	<i>TrpP</i>	−0.1	WP_003233236	<i>TrpP</i>	3.5
WP_003230608	<i>TrpA</i>	1.1	WP_124058510	<i>TrpA</i>	1.9
WP_029725858	<i>PatB</i>	−1.4	WP_153256127	<i>DhaS</i>	0.8
			WP_024571520	<i>PatB</i>	2.5
			WP_021076225	<i>iaaH</i>	−1.0
<b>Terpenoids</b>					
AGA20733	<i>IspF</i>	−1.2	WP_181219684	<i>fni</i>	1.8
AGA24047	<i>Dxr</i>	−2.0	AGA20733	<i>IspF</i>	1.3
WP_003235019	<i>IspD</i>	0.0	AGA24047	<i>Dxr</i>	−1.1
WP_032722383	<i>fni</i>	3.8	WP_003235520	<i>IspD</i>	0.3
<b>2,3-BD</b>					
6IE0-A	<i>R-BDH</i>	2.3	WP_029946299	<i>bdhA</i>	−2.1
<b>Serine protease</b>					
WP_014479598	<i>Isp</i>	4.8	WP_024572446	<i>AprX</i>	5.6
WP_032721588	<i>AprX</i>	−1.0	WP_014479598	<i>Isp</i>	4.0
WP_015250812	<i>HtrC</i>	−1.5	WP_015250812	<i>HtrC</i>	1.3
WP_032722717	<i>Vpr</i>	3.1	WP_134982250	<i>Vpr</i>	4.9
			WP_015382840	<i>TLS</i>	3.6
<b>Bacillibactin</b>					
WP_019712937	<i>DhbC</i>	−0.8	WP_014480725	<i>DhbA</i>	3.1
WP_019712934	<i>DhbF</i>	0.0	WP_029946202	<i>DhbE</i>	1.6
			WP_106073425	<i>DhbB</i>	1.5
			WP_042974556	<i>DhbC</i>	2.6
			WP_185183915	<i>DhbF</i>	2.5
			WP_129092200	<i>Btr</i>	3.9
			KAF1340485.1	<i>DhbA</i>	3.9
<b>EPS</b>					
WP_194395382	<i>EpsB</i>	0.0	WP_194395382	<i>EpsB</i>	2.9
WP_032722561	<i>EpsE</i>	−1.3	WP_181220166	<i>EpsC</i>	3.2
WP_015714749	<i>EpsG</i>	−1.2	WP_128993438	<i>EpsE</i>	3.0
WP_003246541	<i>EpsK</i>	1.1	WP_015714749	<i>EpsG</i>	2.8
			WP_003234384	<i>EpsK</i>	3.2
			WP_124059006	<i>pdeH</i>	1.6
			WP_166443901	<i>sugtrans</i>	4.2
			WP_123373775	<i>EpsI</i>	1.7
<b>Spermidine</b>					
WP_003227543	<i>speE</i>	−0.2	WP_003227543	<i>speE</i>	1.1

FC represents the fold change in expression levels during the stationary phase as compared to the log phase.

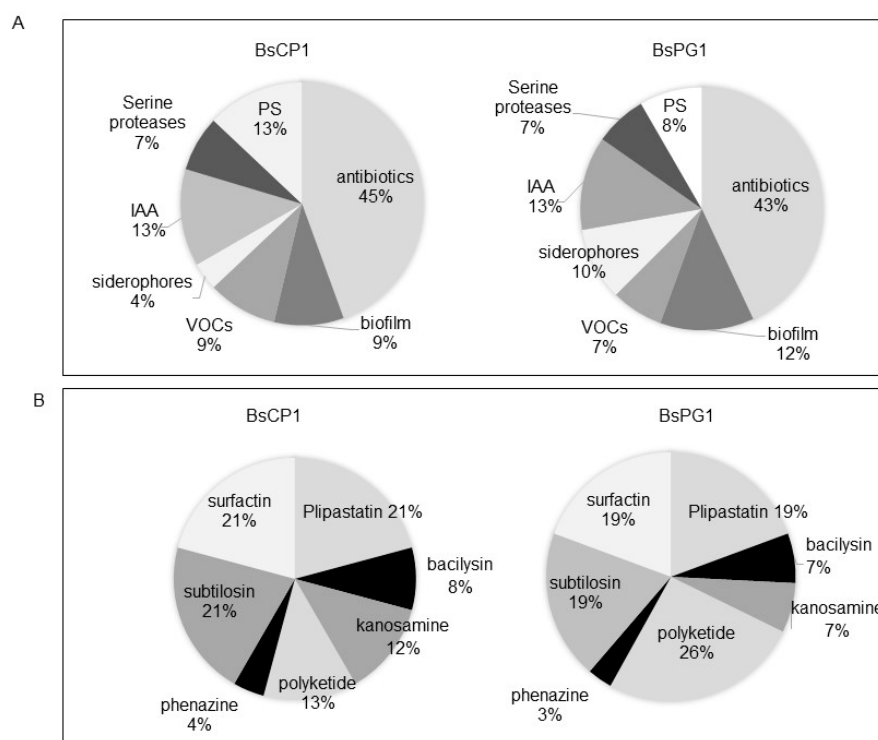


**Figure 2.** Genes associated with plant growth-promoting traits in BsCP1 and BsPG1 genome. These genes were classified into seven groups based on their annotated functions (A). Genes involved in antibiotic synthesis were further subgrouped into seven categories (B). PS: phosphate solubilization. VOCs: volatile organic compounds.

The genes identified from the transcriptome studies of BsCP1 and BsPG1 were classified as up-regulated when they had a  $\text{Log}_2[\text{FC}]$  value greater than or equal to 1.0 and as not up-regulated when the  $\text{Log}_2[\text{FC}]$  value was less than 1.0. The FC represents the fold change in expression levels during the stationary phase compared to the log phase. For these genes involved in synthesis of antibiotic compounds, the expression of genes responsible for synthesis of plipastatin, bacilysin, kanosamine, and phenazine exhibited similar patterns between BsCP1 and BsPG1 (Figure 3). However, there were distinct differences in gene expression patterns between the two bacterial strains regarding the synthesis of polyketide, subtilosin, and surfactin. In BsCP1, most genes involved in subtilosin synthesis were upregulated during the stationary phase. However, in BsPG1, subtilosin-synthesizing genes were not up-regulated. Distinct transcriptional patterns were observed for surfactin-synthesizing genes: while four genes in BsCP1 were not up-regulated, all six genes in BsPG1 were up-regulated. Both bacterial strains exhibited similar expression patterns for genes related to phosphate solubilizing activity, as well as the synthesis of IAA and terpenoids (Figure 3). For serine protease synthesizing genes, 50% and 100% of them were up-regulated in BsCP1 and BsPG1, respectively. In the context of bacillibactin synthesis during the stationary phase, BsCP1 had two genes: one with unchanged expression and another with reduced expression. In contrast, all seven genes in this category for BsPG1 were upregulated, each displaying a  $\text{Log}_2[\text{FC}]$  value greater than 1.0. For EPS synthesis, one out of four genes in BsCP1 showed increased expression. However, in BsPG1, eight genes exhibited upregulated expression. A single gene associated with 2,3-BD synthesis was upregulated in BsCP1 and not up-regulated in BsPG1. Similarly, one gene related to spermidine synthesis was identified in both strains; it was not up-regulated in BsCP1 but upregulated in BsPG1. The transcriptome analysis results reveal noticeable differences in transcription profiles between BsCP1 and BsPG1. This includes genes associated with the synthesis of antibiotics (e.g., polyketide, subtilosin, and surfactin), serine protease, bacillibactin, and EPS.

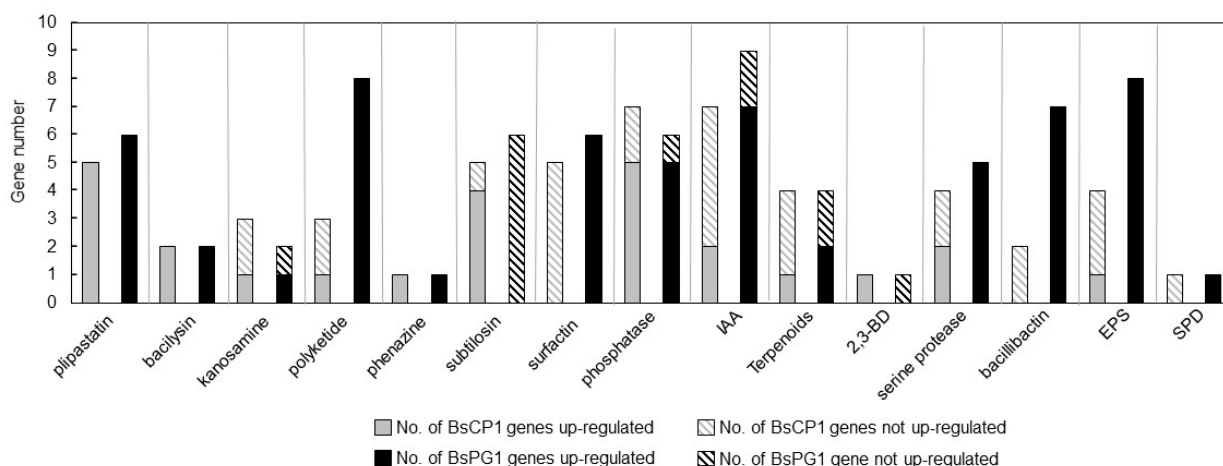


**Figure 3.** Comparison of genes derived from transcriptome analyses. Genes identified from the transcriptome analysis of BsCP1 and BsPG1, associated with the synthesis of metabolites that correlate with plant growth promotion, were categorized based on their fold change in expression levels during the stationary phase compared to the log phase. Genes with a  $\text{Log}_2[\text{FC}]$  value of 1.0 or higher were considered up-regulated. These are represented by a gray solid block for BsCP1 genes and a black solid block for BsPG1 genes. Genes with  $\text{Log}_2[\text{FC}]$  values less than 1.0 are represented by a gray striped block for BsCP1 genes and a black striped block for BsPG1 genes. These values signify genes that are not up-regulated in expression during the stationary phase compared to the log phase.

### 2.3. Biochemical Properties of BsCP1 and BsPG1

*Bacillus* species produce various metabolites that can act as biocontrol agents against phytopathogens [38]. After a seven-day coculture, BsCP1 and BsPG1 were able to suppress approximately 44% and 52% of the mycelial growth of *Foc TR4*, respectively (Figure 4A). *Foc TR4* is a pathogen for causing banana *Fusarium* wilt [39]. However, when cultured on media separated from *Foc TR4*, the volatile metabolites produced by these two *B. subtilis* strains were observed to change the mycelia morphology, but had no effect on reducing the mycelial growth of *Foc TR4* (Figure 4B). Improving phosphate solubilization in the soil is a well-recognized mechanism for promoting plant growth mediated by PGPR [40]. BsPG1 displayed higher phosphate solubilizing activity than BsCP1 (Figure 4C). Both bacterial strains also produced between 0.8 to 5.6 ppm of IAA over a three-day culture period (Figure 4D). Despite this, both bacterial strains produced significant amounts of extracellular polymeric substances, EPS, with BsPG1 producing approximately 2.5 times more EPS compared to BsCP1 (Figure 4E). On the medium containing skim milk, similar clear zones were visible surrounding the colonies of BsCP1 and BsPG1, suggesting comparable levels of extracellular protease activity in both bacterial strains (Figure 4F). However, these strains exhibited different molecular patterns of extracellular protease in zymogram electrophoresis gel (Figure 4G). Based on the results of the transcriptome analysis and physiological characterization, BsPG1 was observed to have stronger transcriptional regulation for EPS synthesis genes. Correspondingly, BsPG1 accumulated a higher amount of EPS in its culture compared to BsCP1.

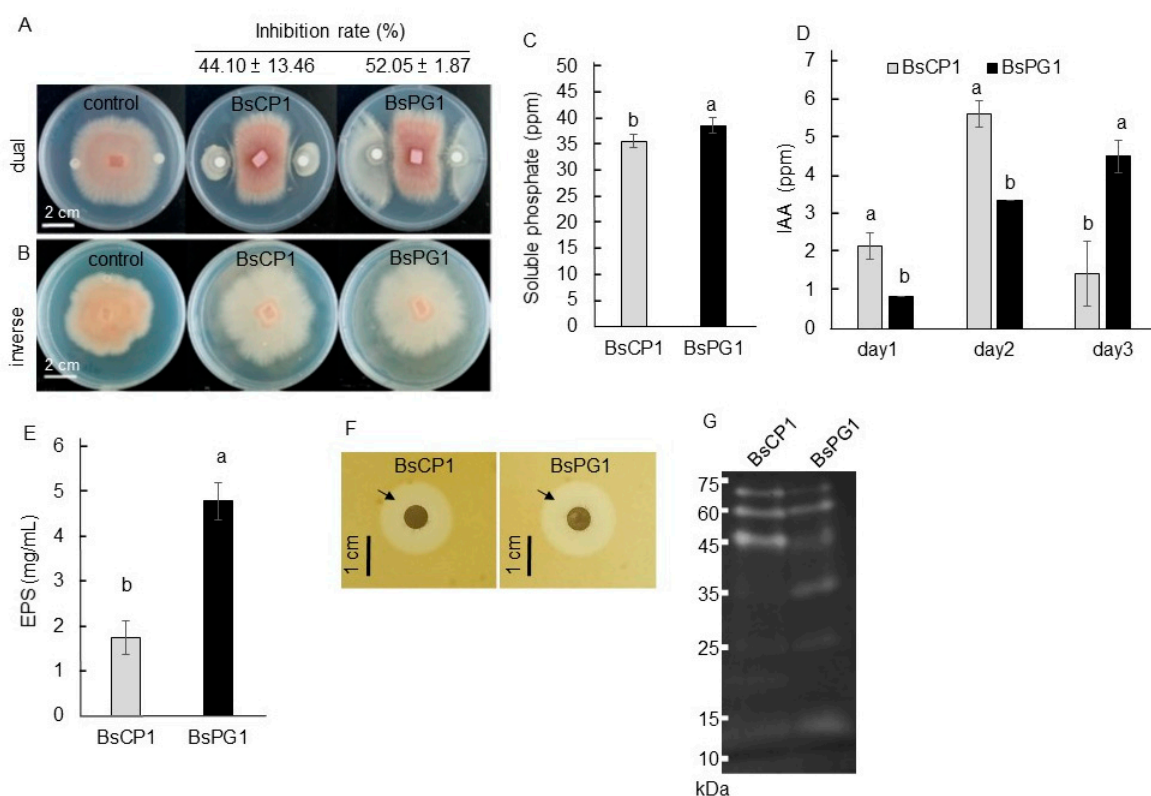


**Figure 4.** Physiological properties of strains BsCP1 and BsPG1. Both bacterial strains produced diffusible metabolites to suppress the mycelial growth of *Foc* TR4 (A). Volatile compounds produced by both bacterial strains altered the mycelial growth of *Foc* TR4 (B). Phosphate solubilizing activity was detected in the bacterial culture (C). IAA concentrations detected in bacterial culture (D). Exopolysaccharides (EPS) were produced by the bacterial strains (E). Clear zones (indicated by arrows) surrounding the bacterial colonies suggest protease activity (F). Zymogram gel was used to detect extracellular proteases on a native gel electrophoresis, using casein as a substrate (G). Values in each histogram represent the mean of three replicates  $\pm$  SD. In histograms C, D, and E, different letters indicate statistical significance at  $p = 0.05$ .

#### 2.4. BsCP1 and BsPG1 Affected Growth of *Arabidopsis* Seedlings

Three-day-old *Arabidopsis* seedlings were co-cultured with BsCP1 and BsPG1 for 7 days. Both bacterial strains increased root branching and increased the number of lateral roots (Figure 5A). Consistently, the soil-grown *Arabidopsis* plants exhibited increased size and gained more fresh weight when treated with BsCP1 and BsPG1 (Figure 5B). Likewise, *Arabidopsis* seedlings treated with BsCP1 and BsPG1 showed increased lignin deposition (Figure 5C). Moreover, increased  $H_2O_2$  accumulation was observed in the tissues treated with both BsCP1 and BsPG1, with BsPG1 inducing higher levels of  $H_2O_2$  compared to BsCP1 (Figure 5D). However, the APX activity in BsCP1- and BsPG1-treated tissues was increased by 2.1-fold and 6.1-fold, respectively, compared to the control (Figure 5E). In contrast, the POD activity in BsCP1- and BsPG1-treated tissues was increased by 2.8-fold and decreased by 0.44-fold, respectively, compared to the control (Figure 5F). These results indicate that BsCP1 exhibited similar effects on activating the enzyme activities of APX and POD. However, BsPG1 had a strong effect on stimulating APX activity while reducing the activity of POD.

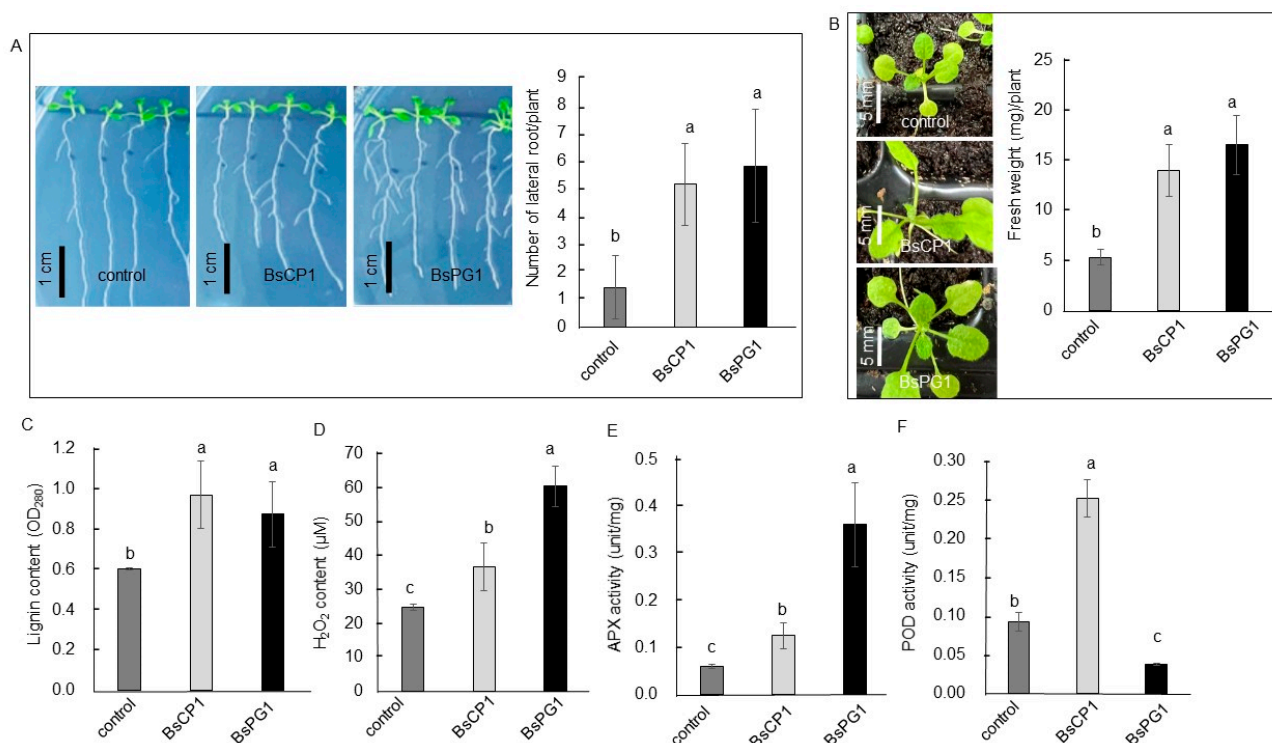


**Figure 5.** Physiological responses of *Arabidopsis* seedlings toward BsCP1 and BsPG1 treatment. Root architecture and lateral root number in seedlings cocultured with BsCP1 and BsPG1 inoculants for seven days (A). Soil-grown seedlings were treated with BsCP1 and BsPG1 once a week. After three weeks of treatment, the seedlings' growth conditions and changes in fresh weight were analyzed (B), as well as their lignin content (C), H<sub>2</sub>O<sub>2</sub> content (D), APX activity (E), and POD activity (F) in the leaves. Values in each histogram represent the mean of three replicates  $\pm$  SD. Different letters within the histograms represent statistical significance at a *p*-value of 0.05.

### 2.5. Differential Effects of BsCP1 and BsPG1 on Enhancing Plant Stress Resilience

Three-week-old *Arabidopsis* seedlings were pretreated with BsCP1 and BsPG1 inoculants and examined for drought stress tolerance by withholding water supply for 7 days. The seedlings that received BsCP1 and BsPG1 pretreatment exhibited a lower number of wilted seedlings, demonstrating a higher percentage of surviving plants (Figure 6A). In the post-drought period, the seedlings with BsCP1 and BsPG1 pretreatment displayed larger plant sizes and gained more fresh weight compared to the control seedlings (Figure 6B). The BsPG1-pretreated seedlings exhibited an elevated starch accumulation, whereas the BsCP1-treated seedlings did not show such an increase (Figure 6C). Starch serves as a storage form of photosynthate, and it is released under various abiotic stresses to act as an energy source and can alleviate stress damage [41]. Drought resistance is correlated with a higher accumulation of starch in common bean cultivars [42].

To analyze heat stress tolerance, two-week-old *Arabidopsis* seedlings were pretreated with BsCP1 and BsPG1 inoculants and subsequently exposed to a temperature of 45 °C for 20 min. Twenty-four hours after returning to the normal growth temperature of 23 °C, seedlings with the BsPG1 pretreatment showed a reduced number of wilted seedlings, indicating a higher percentage of survival compared to the control seedlings. However, the survival rate of seedlings pretreated with BsCP1 was similar to that of the control seedlings (Figure 7A). In the post-heat stress period, seven days after being cultured at 23 °C, seedlings with pretreatments exhibited larger plant sizes and gained more fresh weight. Specifically, the seedlings pretreated with BsPG1 showed a greater increase in fresh weight compared to the BsCP1-pretreated seedlings (Figure 7B). Furthermore, there was a significant increase in starch accumulation observed in both the BsCP1 and BsPG1 pretreated seedlings compared to the control seedlings. Importantly, the increment in

starch accumulation was higher in the seedlings pretreated with BsPG1 compared to those pretreated with BsCP1 (Figure 7C).

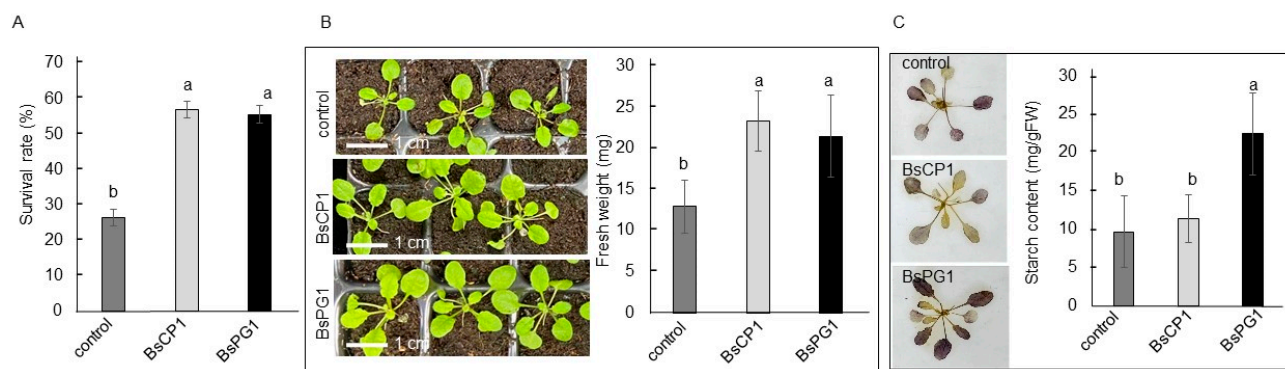


**Figure 6.** Drought stress tolerance induced by BsCP1 and BsPG1. Three-week-old seedlings treated with BsCP1 and BsPG1 had watering withheld for seven days. After resuming growth at 23 °C for five days, the drought-stressed seedlings were investigated for survival rate (A), seedling size and fresh weight (B), and starch accumulation by staining and quantitative measurement (C). Values in each histogram represent the mean of three replicates  $\pm$  SD. Different letters within the histograms represent statistical significance at a  $p$ -value of 0.05.

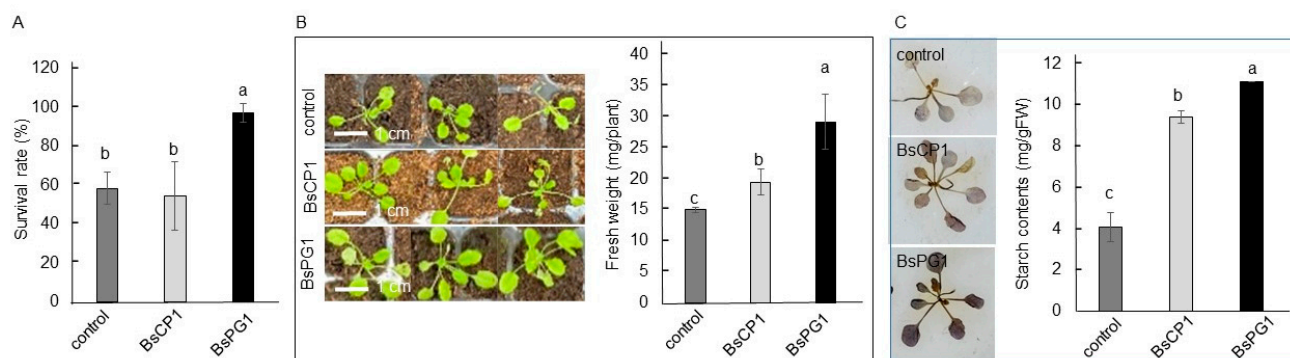


**Figure 7.** Heat stress tolerance induced by BsCP1 and BsPG1. Two-week-old *Arabidopsis* seedlings treated with BsCP1 and BsPG1 were exposed to 45 °C for 20 min. Twenty-four hours after returning to 23 °C growth condition, the survival rate of the heated-stressed seedlings was analyzed (A). Seven days after recovering at 23 °C, seedlings were investigated for seedling size and fresh weight (B), and starch accumulation by staining and quantitative measurement (C). Values in each histogram represent the mean of three replicates  $\pm$  SD. Different letters within the histograms represent statistical significance at a  $p$ -value of 0.05.

Copper is one of the major heavy metal pollutants found in soil. Although a trace amount of copper is necessary for plant growth, an excessive quantity of copper induces oxidative stress, subsequently resulting in toxicity to plant biomass and chlorophyll content [43]. The response of seedlings to 200  $\mu$ M CuSO<sub>4</sub> was analyzed to determine the effects of BsCP1 and BsPG1 on improving heavy metal tolerance. As shown in Figure 8A, when exposed to 200  $\mu$ M CuSO<sub>4</sub>, the control seedlings displayed symptoms of heavy metal damage in plants, such as leaf chlorosis and growth inhibition [44]. The control seedlings exhibited a 15.9% reduction in chlorophyll content and a 44.6% reduction in plant fresh weight under the 200  $\mu$ M CuSO<sub>4</sub> treatment (Figure 8B,C). The seedlings pretreated with BsCP1 showed a moderate enhancement in heavy metal tolerance, with a decrease in chlorophyll content by 7.6% and plant fresh weight by 24.4%. However, the seedlings pretreated with BsPG1 exhibited a stronger increase in copper stress tolerance, displaying only a minor reduction in chlorophyll content (0.7%) and plant fresh weight (4.9%).

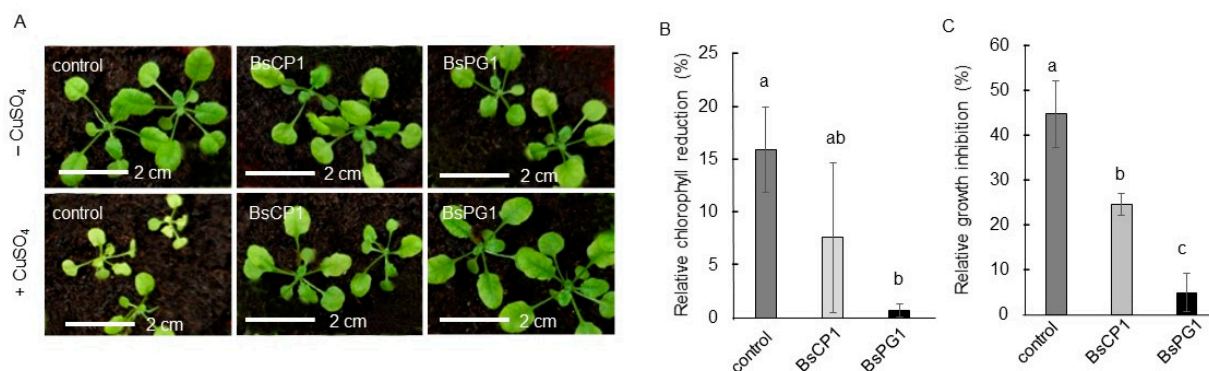


**Figure 8.** Analysis of copper stress tolerance induced by BsCP1 and BsPG1. Two-week-old *Arabidopsis* seedlings treated with BsCP1 and BsPG1 were exposed to 200  $\mu\text{M}$   $\text{CuSO}_4$ . After three exposures, obvious stunting of growth and leaf bleaching were observed in the control seedlings (A). The relative chlorophyll reduction (B) and growth inhibition rate (C) were investigated. Values in each histogram represent the mean of three replicates  $\pm$  SD. In histograms B and C, different letters represent statistical significance at a  $p$ -value of 0.05.

### 2.6. BsCP1 and BsPG1 Altered Expression of Genes Associated with Hormone Signals

The treatments of BsCP1 and BsPG1 exhibited differential effects on improving the stress response of *Arabidopsis* seedlings. To investigate the underlying mechanisms, we examined the expression of genes associated with the SA, JA, and ABA signaling pathways using qPCR analysis. The functions of *isochorismate synthase 1 (ICS1)*, *enhanced disease susceptibility 1 (EDS1)*, and *CAM-binding protein 60-like G (CBP60G)* are involved in the synthesis and perception of SA [45–47]. The expression of all three genes was induced more than two-fold by BsCP1 and BsPG1 (Figure 9A). qPCR examined the expression of three genes involved in the JA synthesis and signaling pathway, including *oxophytodieneate-reductase 3 (OPR3)*, *lipoxygenase 1 (LOX1)*, and *MYC2* [48–50]. The results show that treatment with BsCP1 resulted in a 2.1-fold increase in *OPR3* expression, a 2.4-fold increase in *LOX1* expression, and a 1.8-fold increase in *MYC2* expression. Conversely, treatment with BsPG1 led to a more substantial induction of gene expression associated with the JA signaling pathway, with all three genes showing an increase of more than two-fold in expression following BsPG1 exposure (Figure 9B). qPCR was also used to examine the expression of genes implicated in ABA synthesis and signaling transduction including *short-chain dehydrogenase reductase 4 (SDR4)*, *nine-cis-epoxycarotenoid dioxygenase 3 (NCED3)*, and *ABA insensitive 5 (ABI5)* [51–53]. The results demonstrate that BsPG1 treatment led to a 2.2-fold, 2.1-fold, and 2.9-fold increase in *SDR4*, *NCED3*, and *ABI5* expression, respectively. In contrast, following BsCP1 treatment, the expression levels of *SDR4*, *NCED3*, and *ABI5* showed respective fold changes of 1.3, 0.36, and 0.87 compared to the control (Figure 9C). This result suggests that BsPG1 serves as a positive regulator of the ABA signaling pathway in *Arabidopsis*. However, this regulatory role was not evident for BsCP1.

Treatment using BsCP1 and BsPG1 enhanced tolerance toward various abiotic stress. The expression of genes involved in the regulatory network of abiotic stress responses such as drought and heat and oxidative stress induces the expression of *DREB2A* [54,55]. Likewise, *ZAT12* performs a role in responding to various abiotic stresses and oxidative stress [56]. Treatment with BsCP1 and BsPG1 increased the expression of both transcription factors (Figure 9D). BsCP1 treatment resulted in a 3.2-fold increase in *DREB2A* expression and a 10.2-fold increase in *ZAT12* expression. Similarly, BsPG1 treatment led to an 8.3-fold increase in *DREB2A* expression and a 2.3-fold increase in *ZAT12* expression. *Ascorbate peroxidase 1 (APX1)* encodes a cytosolic form of APX playing a protective role for chloroplast under oxidative stress [57]. *Glutathione peroxidase 7 (GPX7)* is a chloroplast form of GPX [58]. BsCP1 increased the expression of *APX1* by 2.7-fold and *GPX7* by 7.5-fold. BsPG1 increased *APX1* expression by 6.7-fold, but suppressed *GPX7* expression, showing a relative fold change of less than 1.0 (Figure 9D). *Delta-pyrroline-5-carboxylate synthase 1 (P5CS1)* is

involved in the synthesis of proline, acting as a osmoprotectant under abiotic stress [59]. *Chlorophyll a/b binding protein 1 (CAB1)* functions in the light harvesting of photosystem II. This protein affects plant photosynthesis and fitness [60]. BsCP1 induced expression of CAB1 by 2.2-fold but failed to increase the amount of *P5CS1* transcription. BsPG1 showed significant induction for the expression of *P5CS1* and *CAB1* (Figure 9D).

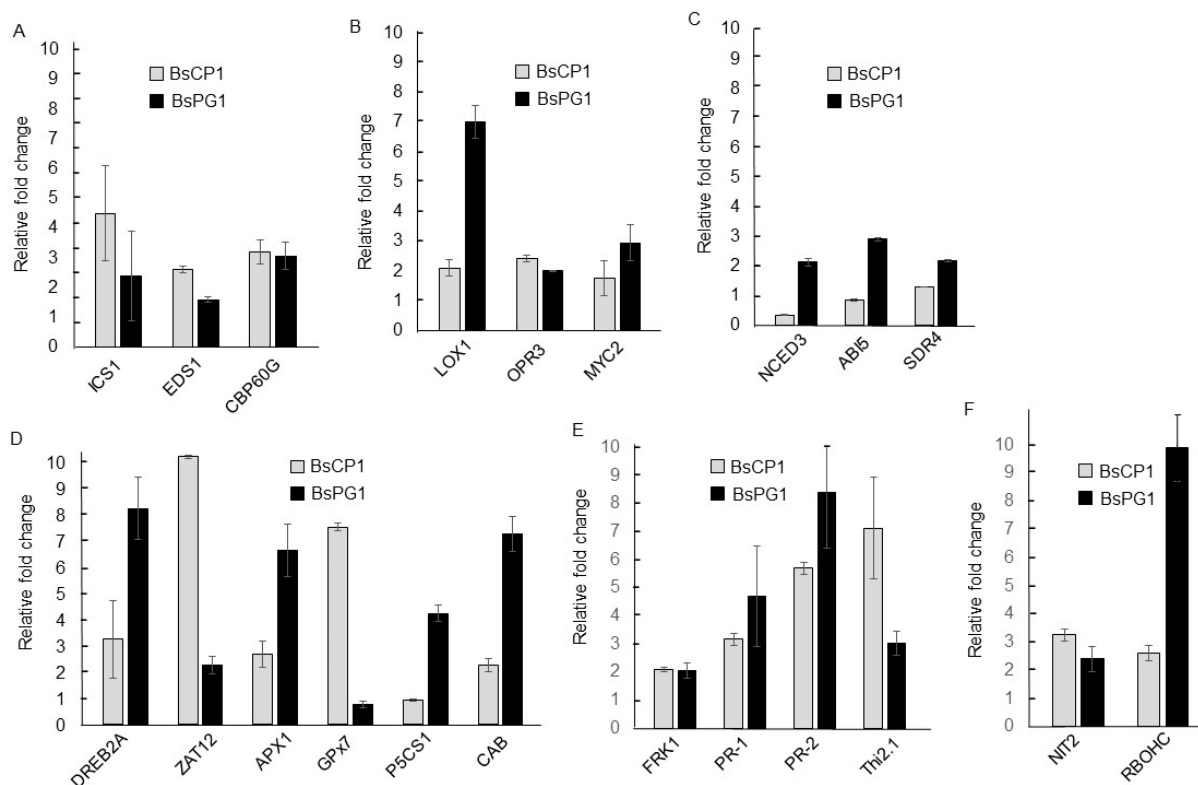


**Figure 9.** *Arabidopsis* gene expression altered by BsCP1 and BsPG1. Changes in gene expression were detected via qPCR analysis using total RNA prepared from whole seedlings treated with BsCP1 and BsPG1. Genes associated with various pathways were investigated, including (A) SA signaling pathway: *isochorismate synthase 1 (ICS1)*, *enhanced disease susceptibility 1 (EDS1)*, and *CAM-binding protein 60-like G (CBP60G)*. (B) JA signaling pathway: *oxophytodienoate-reductase 3 (OPR3)*, *lipoxygenase 1 (LOX1)*, and *MYC2*. (C) ABA signaling pathway: *short-chain dehydrogenase reductase 4 (SDR4)*, *nine-cis-epoxycarotenoid dioxygenase 3 (NCED3)*, and *ABA insensitive 5 (ABI5)*. (D) Abiotic stress response: *DREB2A*, *ZAT12*, *ascorbate peroxidase 1 (APX1)*, *glutathione peroxidase 7 (GPX7)*, *delta-pyrroline-5-carboxylate synthase 1 (P5CS1)*, and *chlorophyll a/b binding protein 1 (CAB1)*. (E) Disease resistance: *flg22-induced receptor-like kinase 1 (FRK1)*, *pathogenesis-related (PR) protein 1 (PR-1)*, *PR-2*, *PR-3*, and *thionin 2.1 (Thi2.1)*. (F) Root development: *nitrilase 2 (NIT2)* and *NADPH oxidase/respiratory burst oxidase homolog C (RBOHC)*.

*flg22-induced receptor-like kinase 1 (FRK1)* is a marker gene for elicitor response [61]. This gene is implicated in disease resistance that is induced by the presence of microbe-associated molecular patterns (MAMPs) [62]. SA and JA are two important plant metabolites to induce the expression of *pathogenesis-related (PR) proteins*, of which *PR-1* and *PR-2* are considered as the marker genes of the SA-induced signaling pathway [63]. However, the expression of *PR-3* and *thionin 2.1 (Thi2.1; PR-13)* is controlled by the JA signal [64,65]. Both BsCP1 and BsPG1 induced expression of *FRK1*, *PR-1*, *PR-2* and *Thi2.1* more than two-fold (Figure 9E).

*Nitrilase 2 (NIT2)* participates in the conversion of indole-3-acetonitrile into the phytohormone IAA, a crucial regulator in the development of lateral roots [2]. The enzyme activity of the NADPH oxidase/respiratory burst oxidase homolog (RBOH) is involved in localized production of oxidative bursts, which regulate plant development and stress responses [66]. ROS produced by RBOHC play roles in regulating root response in developmental stages and

environmental conditions and in controlling the growth of primary roots and root hairs [67,68]. Both BsCP1 and BsPG1 increased transcripts of *NIT2* and *RBOHC* more than two-fold. Moreover, BsPG1 exerted a strong effect on gene induction of *RBOHC* (Figure 9F).

### 3. Discussion

Plant roots secrete various metabolites that act as nutrient sources and environmental signals for rhizosphere bacteria [69]. The composition of these root exudates depends on factors such as the genetic makeup of the plant species, its developmental stage, nutrient availability, and prevailing environmental conditions. Consequently, these exudates can significantly shape the microbial community within the rhizosphere [34]. This study examined the transcription profiles of genes related to plant growth-promoting traits in two *B. subtilis* strains isolated from different sources. *B. subtilis* is renowned for its ability to produce a wide array of metabolites with antimicrobial properties [70]. Our findings reveal that both bacterial strains expressed a substantial number of genes that are linked to the synthesis of antibiotic compounds including plipastatin, bacilysin, kanosamine, polyketide, phenazine, subtilosin, and surfactin. However, these two bacterial strains exhibited differential transcriptional regulation for certain antibiotic synthesis genes, including those involved in the synthesis of polyketide, subtilosin, and surfactin. Consistently with this, a previous study showed that *B. subtilis* strains sourced from different ecological sites may have distinct antibiotic profiles [35]. Our transcriptome analysis identified genes tied to the production of seven antimicrobial metabolites in BsCP1 and BsPG1. Among these, the antifungal activities of plipastatin and surfactin have been validated in previous studies [35,71]. Our results show that BsCP1 and BsPG1 exhibit similar levels of antifungal activity against the pathogen of banana *Fusarium* wilt. The genes responsible for plipastatin synthesis were dominant in both BsCP1 and BsPG1. However, BsPG1 displayed positive transcriptional regulation for surfactin-synthesizing genes, while BsCP1 showed negative transcriptional regulation for these gene expressions. A study by Kiesewalter et al. [35] highlighted the effectiveness of plipastatin in inhibiting the growth of *Fusarium* spp. mycelia. Thus, plipastatin is likely the primary factor responsible for the antifungal efficacy against the *Foc* TR4 pathogen observed in both strains.

The transcriptome data revealed similar transcription profiles for both IAA-synthesizing genes and the genes encoding enzymes responsible for phosphate solubilization in BsCP1 and BsPG1. Consistently with this, both bacterial strains were confirmed to produce IAA and exhibit phosphate solubilizing activity. The application of both bacterial strains to *Arabidopsis* seedlings resulted in increased root branching and stimulated seedling growth. Moreover, at the transcription level, BsCP- and BsPG1 treatment increased the expression of *NIT2*, which is involved in IAA synthesis, as well as *RBOHC*, which plays a role in root hair development by modulating the ROS signal [72,73]. IAA production and phosphate solubilizing activity represent two important traits in PGPR bacterial strains that promote plant growth [74]. Thus, the activities related to IAA production and phosphate solubilization may play a part in the plant growth-promoting effect mediated by BsCP1 and BsPG1. Furthermore, BsCP1 and BsPG1 are capable of generating bioactive VOCs. This is evidenced by the transcriptional control of genes linked to the production of terpenoids and 2,3-BD, as well as their ability to produce volatile substances that affect fungal growth. Although showing polymorphic zymogram patterns for extracellular proteases, these two bacterial strains showed similar extracellular protease activity on the milk-containing medium. At the transcriptional level, treatments with both bacterial strains elevated the expression of genes associated with the SA and JA signaling pathways, as well as genes related to induced disease resistance, such as *FRK1* and *PR* genes. Microbial VOCs have been shown to enhance plant tolerance against both abiotic and biotic stress by activating the SA and JA signaling pathways [75]. Ling et al. [76] demonstrated the antimicrobial activity of microbial serine proteases. Additionally, serine proteases derived from rhizobacteria have been observed to activate plant immune responses and modify cell wall lignification [77]. Studies have shown the significance of SA and JA signaling in mitigating plant oxidative

stress, thereby enhancing stress tolerance [24,27]. Therefore, metabolites and enzymes like VOCs and serine proteases from BsCP1 and BsPG1 could play a pivotal role in triggering the SA and JA signaling pathways. These activations can bolster antioxidant defenses and fortify plants against challenges such as drought, heat, and copper stress.

BsCP1 and BsPG1 showed different transcription regulation for genes responsible for the synthesis of bacillibactin and EPS. Bacillibactin is an iron-binding metabolite from the *Bacillus* species. Its role in plant growth is emphasized by facilitating nutrient uptake efficiency and controlling plant disease through its antimicrobial activity and the activation of systemic resistance [78,79]. During the stationary phase, the majority of genes associated with the synthesis of EPS were up-regulated in BsPG1, but not in BsCP1. The discrepancy in gene expression associated with the synthesis of EPS was consistent with the results showing that BsPG1 produced more EPS than BsCP1. EPS is a main component of biofilm and the production of EPS in microorganisms is affected by environmental factors [80]. Research has reported that the production of EPS is necessary for establishing successful symbiosis between nitrogen-fixing bacteria and host plant roots [14,81]. Since BsPG1 was derived from the rhizosphere of peanut plants, it may account for its increased capacity to generate more EPS than BsCP1.

EPS-producing PGPR may enhance plant tolerance to abiotic stress through various mechanisms, such as retaining soil moisture, triggering antioxidant activity, and the accumulation of osmolytes, as well as removing toxic heavy metals [82–84]. Compared to BsCP1, BsPG1 was a stronger inducer for APX activity and gene expression of *APX1*. The critical function of *APX1* within the regulatory network linked to oxidative stress has been established [57]. In this study, treatment with BsPG1 conferred greater tolerance to drought, heat, and copper stress than treatment with BsCP1 did. Increased oxidative damage is a common outcome resulting from drought, heat, and copper stress [16–18]. Given its higher EPS production, BsPG1 might activate APX1 activity more effectively than BsCP1, which could be a crucial factor in alleviating the harmful impacts of various abiotic stresses. Moreover, BsPG1 exhibited a higher efficiency in inducing starch accumulation during the post-drought and post-heat stress periods. Seedlings treated with BsPG1 also displayed reduced chloroplast damage under copper stress. Starch serves as a storage form of the photosynthetic product. Remobilizing starch to release energy can assist plants in alleviating stress damage [85]. Sugars released from starch under abiotic stress conditions function not only as energy sources but also act as osmoprotectants against osmotic stress [86]. Elevated levels of starch have been detected in *Arabidopsis* leaf tissues when exposed to temperature and osmotic stress conditions [87–89]. The ABA signal is a positive regulator of starch metabolism in maize and rice [90,91]. In *Arabidopsis*, the expression of ADP-glucose pyrophosphorylase (AGPase), a key enzyme involved in starch synthesis, is stimulated by sucrose [92]. Furthermore, ABA has the ability to enhance starch synthesis driven by sucrose [93]. Exogenous ABA has been reported to induce the expression of genes involved in starch synthesis, leading to increased starch accumulation in grapevine cuttings [94]. Consistently, our qPCR results reveal that BsPG1 could activate *Arabidopsis* genes involved in ABA synthesis, such as *NCED3* and *SDR4*, as well as those related to ABA perception like *ABI5*. However, the expression of these genes was not up-regulated in seedlings treated with BsCP1. *P5CS1* is involved in the synthesis of the osmolyte proline [95]. The *P5CS* transcript is induced by drought and salinity stress and the presence of ABA. Additionally, *P5CS* gene activation in seedlings under salt stress is negated in the ABA-deficient mutant [96]. In line with this, only BsPG1 up-regulated the expression of *P5CS1*, while BsCP1 had no effect on its expression. Thus, BsPG1 might significantly enhance abiotic tolerance by modulating ABA signaling in *Arabidopsis* seedlings. The superior EPS production by BsPG1 could stimulate the ABA signaling pathway, which could enhance resistance to stress by minimizing chlorophyll degradation and augmenting the accumulation of starch and proline when subjected to drought, heat, and copper stress.

## 4. Materials and Methods

### 4.1. Bacterial Strain Isolation and Characterization

The soil sample from commercial compost and peanut roots were dissolved in sterilized water. The obtained supernatants were then spotted on the nutrient agar (NA) medium and incubated at 30 °C for overnight. PCR amplification of the genomic DNA from bacterial strains isolated from compost or nodule supernatant was performed using the primers fD1 and rP1 to detect the 16S rDNA sequence. The primers DbhB, DbhE, and DbhF were used for genes associated with bacillibactin synthesis, and sfp was used for surfactin synthesis. PCR amplification began with an initial denaturation at 95 °C for 5 min, followed by 30 cycles of 95 °C for 1 min, annealing at 52 °C for 30 s, and extension at 72 °C for 5 min. This was concluded with a final extension at 72 °C for 3 min. The sequencing results of amplified PCR fragments were analyzed using the Basic Local Alignment Search Tool (BLAST) program [97]. The phylogenetic tree of closely related bacterial strains was constructed using the neighbor-joining algorithm (NJ) in MEGA X software [98]. Primer sequences used for PCR analysis are listed in Supplementary Table S1.

### 4.2. RNA-Seq Analysis

Bacteria were cultured for 4 and 16 h, representing the log and stationary phases, respectively. The cells were collected for RNA extraction using the hot SDS/phenol method as described by Jahn et al. [99]. We subjected 1 µg of total RNA to library construction using the Universal Prokaryotic RNA -Seq library preparation kit (TECAN). Sequencing was performed using a NovaSeq 6000 System (Illumina, San Diego, CA, USA). The quality of RNA-seq raw reads was evaluated using CLC Genomics Workbench 10 software (Qiagen, Germantown, MD, USA). The raw reads were trimmed and assembled using SPAdes (v3.15.3) [100]. The rRNA, tRNA, and open reading frame (ORF) of the protein coding sequence were predicted using RNAmmer (v1.2), tRNAscan-SE (v1.3.1), and the Glimmer program, respectively [101–103]. The ORFs were annotated using NCBI blast software (v.2.2.28+) and the COGs (Clusters of Orthologous Groups) database [104]. The gene ontology (GO) annotation was performed using FastAnnotation, while pathway analysis was conducted through the KEGG Automatic Annotation Server (KAAS) [105,106]. The prediction of pathways and antibiotic gene prediction were carried out using the CARD database [107]. The gene expression values were quantified using FPKM (Fragments Per Kilobases per Million). The differential gene expression between the two time points was determined by dividing the FPKM value of the 16 h culture by that of the 4 h culture.

### 4.3. Analysis of Biochemical Properties of Isolated Bacterial Strains

#### 4.3.1. Antifungal Activity

Detecting the antifungal activity of the nonvolatile and volatile metabolites produced by bacterial strains was performed using methods described by Tsai et al. [33]. In brief, to detect nonvolatile compounds, two filter paper pieces were prepared, each containing 10 µL of bacterial solutions that had been cultured overnight in LB medium at a concentration of  $1 \times 10^8$  CFU/mL, while water was used as a control. These filter papers were placed 3 cm away from a mycelial plug of *Fusarium oxysporum* f. sp. *cubeense* tropical race 4 (*Foc* TR4) on potato dextrose agar (PDA) medium, and the cultures were cocultured for 7 days at 28 °C. To test the antifungal activity of volatile metabolites produced by the bacterial strains, both the fungal pathogen *Foc* TR4 and the bacterial strains were separately grown on Petri dishes containing PDA medium and LB medium, respectively. Subsequently, the plate containing the fungal strain and bacterial strains were positioned face-to-face and cocultured for 7 days at 28 °C. The diameter of the fungal mycelia in the control group and those cocultured with bacterial strains was measured to determine the rate of inhibition of mycelial growth (I) = (1-diameter of mycelia of treatment/diameter of mycelia of control) × 100.

#### 4.3.2. Quantification of Phosphate Solubilization

To quantify the activity of phosphate solubilization, a single colony of the tested bacterial strain was grown in Pilovskaya's (PVK) medium containing 1% glucose, 0.05%  $(\text{NH}_4)_2\text{SO}_4$ , 0.02% NaCl, 0.03% KCl, 0.052%  $\text{FeSO}_4 \cdot 7\text{H}_2\text{O}$ , 0.045%  $\text{MnSO}_4 \cdot 4\text{H}_2\text{O}$ , 0.057%  $\text{MgSO}_4 \cdot 7\text{H}_2\text{O}$ , 0.5%  $\text{Ca}_3(\text{PO}_4)_2$ , and 0.04% yeast extract at 28 °C for 3 days. The bacterial culture was then subjected to centrifugation, and 1 mL of the resulting supernatant was combined with 0.4 mL of Vanadate–Molybdate reagent and 0.6 mL of  $\text{H}_2\text{O}$ . The mixture was then incubated at room temperature for 60 min, and the optical density at 470 nm was recorded. The concentration of solubilized phosphate in the bacterial supernatant was calculated based on a standard curve prepared from various concentrations of  $\text{KH}_2\text{PO}_4$ .

#### 4.3.3. Detection of Indole Acetic Acid (IAA) and Exopolysaccharide (EPS) Production

For the quantification of indole acetic acid (IAA), the tested bacterial strains were cultured in Luria–Bertani (LB) medium containing 2 mM tryptophan for 24, 48, and 72 h at 28 °C. One milliliter of bacterial supernatant was mixed with the Salkowski reagent and incubated at room temperature for 10 min. The absorbance of the mixture was measured at a wavelength of 530 nm to determine the concentration of IAA.

#### 4.3.4. Detection of Exopolysaccharide (EPS) Production

The EPS production of the tested bacterial strains was assessed using the methods described by Nwosu et al. [108]. The bacterial strains were cultured in nutrient broth containing 0.5% peptone, 0.3% yeast extract, and 0.5% NaCl, supplemented with 2% sucrose. After incubating the cultures at 28 °C for 24 h, they were subjected to centrifugation. The resulting supernatants were combined with two volumes of 95% ethanol and incubated overnight at 4 °C. Subsequently, the EPS extracted from the bacterial supernatants was collected via centrifugation and dried for 3 h at 60 °C. The amount of EPS produced by the bacterial strains was determined by measuring the dry weight of the EPS precipitates.

#### 4.3.5. Analysis of Protease Activity

To detect protease activity, a 5  $\mu\text{L}$  aliquot of a bacterial culture with a concentration of  $1 \times 10^8$  CFU/mL was placed on a 5 mm diameter filter paper positioned at the center of a medium containing 5% skim milk and 4% agar. The culture was then incubated at 28 °C for 2 days. The presence of a clear zone around the bacterial colony indicates the presence of protease activity. For the preparation of zymogram analysis, bacterial strains were cultured in a medium containing 1% peptone, 0.5% yeast extract, and 1% skim milk at 28 °C for 3 days. Subsequently, the bacterial cultures were centrifuged to collect the cell-free supernatants. The protease pellets were precipitated by adding ammonium sulfate until reaching 80% saturation. Afterward, the protease pellets were collected through centrifugation, suspended in 50 mM of phosphate buffer at pH 7.0, and subsequently used for zymogram electrophoresis analysis, following the method described by Tsai et al. [33].

#### 4.4. Analysis of Growth-Promoting Effects in *Arabidopsis* Seedlings

Four-day-old seedlings of *Arabidopsis thaliana* (Columbia ecotype) obtained from The Arabidopsis Information Resource (TAIR) were co-cultured with the tested bacterial colonies. These colonies were positioned 4 cm away from the seedlings in 1/2 Murashige and Skoog (MS) medium and then incubated at 23 °C under a 16 h lighting condition. The number of lateral roots in both the control and treated seedlings was recorded after a seven-day co-culture period. Further growth-promoting effects of the tested bacterial strain were observed in *Arabidopsis* seedlings grown in soil. The tested bacterial strain cultured in the LB broth for 16 h was collected via centrifugation and suspended in water to a bacterial density of  $1 \times 10^8$  CFU/mL. The bacterial solution was administered through foliar spraying on 2-week-old *Arabidopsis* seedlings once a week for three successive weeks. In the control, seedlings were treated with water. Twenty seedlings were included in each treatment. The fresh weights of both the control and treated seedlings were recorded, and

lignin was extracted from the tissues of both groups following the methods described by Govender et al. [109]. Briefly, leaf tissues of 0.1 g were extracted in a solution containing 100 mM phosphate buffer (pH 7.4) and 0.5% Triton-100. The obtained pellets were washed with 95% methanol and dried at room temperature. The crude lignin extracts were used for lignin quantification using the thioglycolic acid (TGA) method as described by Bruce and West [110]. To detect H<sub>2</sub>O<sub>2</sub> production, 0.1 g of leaf tissues were extracted in 80% ethanol, and the obtained supernatants were mixed with the ferrous ion oxidation xylenol orange (FOX) reagent as described by DeLong et al. [111]. After incubation for 30 min in the dark, the H<sub>2</sub>O<sub>2</sub> concentrations were determined by measuring the absorbance at 560 nm. The enzyme activity of ascorbate peroxidase (APX) was quantified by extracting 0.1 g of leaf tissues in a solution containing 50 mM potassium phosphate buffer (pH 7.0), 1% polyvinylpyrrolidone (PVP), and 0.1 mM EDTA, as described by Nakano and Asada [112]. The obtained supernatants were mixed with a reaction solution containing 50 mM potassium phosphate buffer (pH 7.0), 0.2 mM EDTA, 0.5 mM ascorbic acid, and 2% H<sub>2</sub>O<sub>2</sub>. APX activity was determined by measuring the absorbance at 290 nm after 5 min of incubation. To detect guaiacol peroxidase (POD) activity, 0.1 g of leaf tissues were extracted in a solution containing 0.1 mM EDTA and 0.2 M potassium phosphate buffer (pH 7.8), as described by Aebi [113]. The obtained supernatants were mixed with a reaction solution containing 1% guaiacol, 40 mM H<sub>2</sub>O<sub>2</sub>, and 100 mM phosphate buffer (pH 7.0). POD activity was quantified by measuring the absorbance at 470 nm after incubation for 10 min. The experiments were conducted three times.

#### 4.5. Analysis of Abiotic Stress Tolerance in *Arabidopsis* Seedlings

##### 4.5.1. Analysis of Drought Stress Tolerance

For the analysis of drought stress tolerance, three-week-old *Arabidopsis* seedlings grown in seedling trays were pretreated with a bacterial suspension of  $1 \times 10^8$  CFU/mL 3 times. After bacterial treatments, watering was withheld from the seedlings for 7 days. The watering was resumed for the drought-stressed seedlings for 5 days. Forty seedlings were included in each treatment. The fresh weight and starch contents were analyzed at the end of 5-day culture. The survival rates of the control and treated seedlings were calculated by dividing seedlings without wilted leaves by total seedling number. Seedling fresh weights and starch contents were measured at the end of the 5-day recovery period. The starch contents were analyzed using a method described by Tsai et al. [114]. Briefly, seedlings were boiled in water for 5 min and then transferred to 80% ethanol for an additional 3-min boiling. For a qualitative assay, 100  $\mu$ L of Lugol's iodine solution was used to stain starch granules in the leaf tissues. To quantify starch content, the solution was mixed with Lugol's iodine solution (Sigma-Aldrich, St. Louis, MI, USA) and the absorbance at 620 nm was measured. The drought stress tolerance analysis was performed in triplicate.

##### 4.5.2. Analysis of Heat Stress Tolerance

To analyze the heat stress response, two-week-old *Arabidopsis* seedlings treated with the tested bacterial strains were exposed to 45 °C for 20 min and then returned to a growth temperature of 23 °C. Each treatment consisted of 40 seedlings. The wilted seedlings were observed after recovery at 23 °C for 24 h to calculate their survival rates. Seedling fresh weights and starch contents were measured at the end of the 7-day recovery period. The starch contents were analyzed using a method described above. The heat stress tolerance analysis was performed in triplicate.

##### 4.5.3. Analysis of Copper Stress Tolerance

For testing plant tolerance to copper stress, two-week-old *Arabidopsis* seedlings were pretreated with bacterial suspension in  $1 \times 10^8$  CFU/mL 3 times, while the control plants were treated with water. One day after the pretreatment, a 20 mL solution of 200  $\mu$ M CuSO<sub>4</sub> was applied to the soil once every two days for a total of three times. Each treatment consisted of 30 seedlings. One day after the final treatment, the fresh weight of both CuSO<sub>4</sub>-

treated and untreated plants was measured. The growth inhibition rate (%):  $(1 - \text{fresh weight of CuSO}_4\text{-treated plants} / \text{fresh weight of water-treated plants}) \times 100$ . The chlorophyll contents of both CuSO<sub>4</sub>-treated and untreated plants were extracted and quantified using a method described by Kurniawan and Chuang [115]. The relative chlorophyll reduction rate (%):  $(1 - \text{chlorophyll content of the CuSO}_4\text{-treated plants} / \text{chlorophyll content of water-treated plants}) \times 100$ . The analysis for copper stress tolerance was conducted three times.

#### 4.6. qPCR Analysis for Arabidopsis Gene Expression

Total RNA was extracted from the leaf and root tissues of 10-day-old *Arabidopsis* seedlings cocultured with the tested bacterial strains for 7 days using the methods described by Lee Downing et al. [116]. cDNA was prepared from 2 µg of total RNA using ImProm-II™ reverse transcriptase (Promega) for qPCR amplification. The amplification was performed using SYBR Green Master Mix in the StepOne™ Real-Time PCR System (Thermo Fisher). The relative gene expression level was calculated using the  $2^{-\Delta\Delta C_t}$  method and the gene expression of *actin 2* (*ACT2*) was used as a reference gene for normalization. The primer sequences used for qPCR analysis are listed in Supplementary Table S1.

#### 4.7. Statistical Analysis

The differences between the treatments were analyzed using the ANOVA procedure in the SAS (3.8) software package. A *p*-value less than 0.05 from the Tukey test was considered to be statistically significant.

### 5. Conclusions

This research investigated two *B. subtilis* bacterial strains sourced from distinct origins. Both strains demonstrated similarities in antimicrobial activity, extracellular protease function, phosphate solubilization, and the production of IAA and VOCs. Yet, differences emerged in their synthesis of bacillibactin and EPS. Both bacterial strains enhanced lateral root development and increased seedling fresh weight; furthermore, they activated the antioxidant activity and plant defense response to increase tolerance against various abiotic stresses. Our results indicate that *B. subtilis* strains with a greater ability to produce EPS show a stronger capacity to enhance plant tolerance to drought, heat, and copper stress. Additionally, strains that generate larger quantities of EPS are capable of triggering the ABA signaling pathway in *Arabidopsis* seedlings. The results of this study suggest that PGPR strains from different ecological sites have significant potential to produce polymorphic metabolites, which can vary in their effects on plant growth and stress response.

**Supplementary Materials:** The following supporting information can be downloaded at: <https://www.mdpi.com/article/10.3390/ijms241813720/s1>.

**Author Contributions:** P.E.C., phylogenetic tree analysis, bacterial characterization, plant experiment, qPCR analysis; Y.-H.W., bacterial characterization; C.-Y.T., plant experiments; I.-H.L., bacterial identification; W.-D.W., providing comments on manuscript preparation; T.-S.T., providing feedback on the experiment and comments on manuscript preparation; H.-w.C., experimental design, data analysis, and manuscript writing. All authors have read and agreed to the published version of the manuscript.

**Funding:** This research was funded by National Science and Technology Council, Taiwan, grant number MOST 111WFA1610040.

**Data Availability Statement:** Not applicable.

**Conflicts of Interest:** The authors declare no conflict of interest.

## References

1. Spaepen, S.; Vanderleyden, J.; Remans, R. Indole-3-acetic acid in microbial and microorganism-plant signaling. *FEMS Microbiol. Rev.* **2007**, *31*, 425–448. [[CrossRef](#)] [[PubMed](#)]
2. De Smet, I.; Vanneste, S.; Inzé, D.; Beeckman, T. Lateral root initiation or the birth of a new meristem. *Plant. Mol. Biol.* **2006**, *60*, 871–887. [[CrossRef](#)]
3. Pantoja-Guerra, M.; Valero-Valero, N.; Ramírez, C.A. Total auxin level in the soil–plant system as a modulating factor for the effectiveness of PGPR inocula: A review. *Chem. Biol. Technol. Agric.* **2023**, *10*, 6. [[CrossRef](#)]
4. Nithyapriya, S.; Lalitha, S.; Sayyed, R.Z.; Reddy, M.S.; Dailin, D.J.; El Enshasy, H.A.; Luh Suriani, N.; Herlambang, S. Production, purification, and characterization of bacillibactin siderophore of *Bacillus subtilis* and its application for improvement in plant growth and oil content in sesame. *Sustainability* **2021**, *13*, 5394. [[CrossRef](#)]
5. Naing, A.H.; Maung, T.T.; Kim, C.K. The ACC deaminase-producing plant growth-promoting bacteria: Influences of bacterial strains and ACC deaminase activities in plant tolerance to abiotic stress. *Physiol. Plant.* **2021**, *173*, 1992–2012. [[CrossRef](#)]
6. Fincheira, P.; Quiroz, A. Microbial volatiles as plant growth inducers. *Microbiol. Res.* **2018**, *208*, 63–75. [[CrossRef](#)] [[PubMed](#)]
7. Avalos, M.; van Wezel, G.P.; Raaijmakers, J.M.; Garbeva, P. Healthy scents: Microbial volatiles as new frontier in antibiotic research? *Curr. Opin. Microbiol.* **2018**, *45*, 84–91. [[CrossRef](#)] [[PubMed](#)]
8. Wu, L.; Li, X.; Ma, L.; Borriss, R.; Wu, Z.; Gao, X. Acetoin and 2,3-butanediol from *Bacillus amyloliquefaciens* induce stomatal closure in *Arabidopsis thaliana* and *Nicotiana benthamiana*. *J. Exp. Bot.* **2018**, *69*, 5625–5635. [[CrossRef](#)]
9. Shi, Y.; Liu, X.; Fang, Y.; Tian, Q.; Jiang, H.; Ma, H. 2, 3-Butanediol activated disease-resistance of creeping bentgrass by inducing phytohormone and antioxidant responses. *Plant Physiol. Biochem.* **2018**, *129*, 244–250. [[CrossRef](#)]
10. Raaijmakers, J.M.; De Bruijn, I.; Nybroe, O.; Ongena, M. Natural functions of lipopeptides from *Bacillus* and *Pseudomonas*: More than surfactants and antibiotics. *FEMS Microbiol. Rev.* **2010**, *34*, 1037–1062. [[CrossRef](#)]
11. Jourdan, E.; Henry, G.; Duby, F.; Dommès, J.; Barthelemy, J.-P.; Thonart, P.; Ongena, M. Insights into the defense-related events occurring in plant cells following perception of surfactin-type lipopeptide from *Bacillus subtilis*. *Mol. Plant Microbe Interact.* **2009**, *22*, 456–468. [[CrossRef](#)]
12. Flemming, H.-C.; Wingender, J.; Szewzyk, U.; Steinberg, P.; Rice, S.A.; Kjelleberg, S. Biofilms: An emergent form of bacterial life. *Nat. Rev. Microbiol.* **2016**, *14*, 563–575. [[CrossRef](#)] [[PubMed](#)]
13. Ilyas, N.; Mumtaz, K.; Akhtar, N.; Yasmin, H.; Sayyed, R.Z.; Khan, W.; Enshasy, H.A.E.; Dailin, D.J.; Elsayed, E.A.; Ali, Z. Exopolysaccharides producing bacteria for the amelioration of drought stress in wheat. *Sustainability* **2020**, *12*, 8876. [[CrossRef](#)]
14. Morcillo, R.J.L.; Manzanera, M. The effects of plant-associated bacterial exopolysaccharides on plant abiotic stress tolerance. *Metabolites* **2021**, *11*, 337. [[CrossRef](#)] [[PubMed](#)]
15. Vacheron, J.; Desbrosses, G.; Bouffaud, M.-L.; Touraine, B.; Moëgne-Loccoz, Y.; Muller, D.; Legendre, L.; Wisniewski-Dyé, F.; Prigent-Combaret, C. Plant growth-promoting rhizobacteria and root system functioning. *Front. Plant Sci.* **2013**, *4*, 356. [[CrossRef](#)] [[PubMed](#)]
16. Yang, X.; Lu, M.; Wang, Y.; Wang, Y.; Liu, Z.; Chen, S. Response mechanism of plants to drought stress. *Horticultrae* **2021**, *7*, 50. [[CrossRef](#)]
17. Ruelland, E.; Zachowski, A. How plants sense temperature. *Environ. Exp. Bot.* **2010**, *69*, 225–232. [[CrossRef](#)]
18. Sytar, O.; Kumar, A.; Latowski, D.; Kuczynska, P.; Strzałka, K.; Prasad, M.N.V. Heavy metal-induced oxidative damage, defense reactions, and detoxification mechanisms in plants. *Acta Physiol. Plant.* **2013**, *35*, 985–999. [[CrossRef](#)]
19. Hasanuzzaman, M.; Nahar, K.; Hossain, S.M.; Mahmud, J.A.; Rahman, A.; Inafuku, M.; Oku, H.; Fujita, M. Coordinated actions of glyoxalase and antioxidant defense systems in conferring abiotic stress tolerance in plants. *Int. J. Mol. Sci.* **2017**, *18*, 200. [[CrossRef](#)]
20. Christmann, A.; Weiler, E.W.; Steudle, E.; Grill, E. A hydraulic signal in root-to-shoot signalling of water shortage. *Plant J.* **2007**, *52*, 167–174. [[CrossRef](#)]
21. Watkins, J.M.; Chapman, J.M.; Muday, G.K. Abscisic acid-induced reactive oxygen species are modulated by flavonols to control stomata aperture. *Plant Physiol.* **2017**, *175*, 1807–1825. [[CrossRef](#)] [[PubMed](#)]
22. Vlot, A.C.; Sales, J.H.; Lenk, M.; Bauer, K.; Brambilla, A.; Sommer, A.; Chen, Y.; Wenig, M.; Nayem, S. Systemic propagation of immunity in plants. *New Phytol.* **2021**, *229*, 1234–1250. [[CrossRef](#)]
23. Alharbi, K.; Alaklabi, A. Alleviation of salinity induced growth and photosynthetic decline in wheat due to biochar and jasmonic acid application involves up-regulation of ascorbate-glutathione pathway, glyoxylase system and secondary metabolite accumulation. *Rhizosphere* **2022**, *24*, 100603. [[CrossRef](#)]
24. Singh, S.; Prakash, P.; Singh, A.K. Salicylic acid and hydrogen peroxide improve antioxidant response and compatible osmolytes in wheat (*Triticum aestivum* L.) under water deficit. *Agric. Res.* **2021**, *10*, 175–186. [[CrossRef](#)]
25. Wang, L.-J.; Fan, L.; Loescher, W.; Duan, W.; Liu, G.-J.; Cheng, J.-S.; Luo, H.-B.; Li, S.-H. Salicylic acid alleviates decreases in photosynthesis under heat stress and accelerates recovery in grapevine leaves. *BMC Plant Biol.* **2010**, *10*, 34. [[CrossRef](#)]
26. Khan, M.I.R.; Iqbal, N.; Masood, A.; Per, T.S.; Khan, N.A. Salicylic acid alleviates adverse effects of heat stress on photosynthesis through changes in proline production and ethylene formation. *Plant Signal. Behav.* **2013**, *8*, e26374. [[CrossRef](#)]
27. Su, Y.; Huang, Y.; Dong, X.; Wang, R.; Tang, M.; Cai, J.; Chen, J.; Zhang, X.; Nie, G. Exogenous methyl jasmonate improves heat tolerance of perennial ryegrass through alteration of osmotic adjustment, antioxidant defense, and expression of jasmonic acid-responsive genes. *Front. Plant Sci.* **2021**, *12*, 664519. [[CrossRef](#)] [[PubMed](#)]

28. Ryu, C.-M.; Farag, M.A.; Hu, C.-H.; Reddy, M.S.; Kloepper, J.W.; Paré, P.W. Bacterial volatiles induce systemic resistance in *Arabidopsis*. *Plant Physiol.* **2004**, *134*, 1017–1026. [[CrossRef](#)]
29. Le Mire, G.; Siah, A.; Brisset, M.-N.; Gaucher, M.; Deleu, M.; Jijakli, M.H. Surfactin protects wheat against *Zymoseptoria tritici* and activates both salicylic acid- and jasmonic acid-dependent defense responses. *Agriculture* **2018**, *8*, 11. [[CrossRef](#)]
30. Karatan, E.; Michael, A.J. A wider role for polyamines in biofilm formation. *Biotechnol. Lett.* **2013**, *35*, 1715–1717. [[CrossRef](#)]
31. Zhou, C.; Ma, Z.; Zhu, L.; Xiao, X.; Xie, Y.; Zhu, J.; Wang, J. Rhizobacterial strain *Bacillus megaterium* BOFC15 induces cellular polyamine changes that improve plant growth and drought resistance. *Int. J. Mol. Sci.* **2016**, *17*, 976. [[CrossRef](#)]
32. Gomez, M.Y.; Schroeder, M.M.; Chieb, M.; McLain, N.K.; Gachomo, E.W. *Bradyrhizobium japonicum* IRAT FA3 promotes salt tolerance through jasmonic acid priming in *Arabidopsis thaliana*. *BMC Plant Biol.* **2023**, *23*, 60. [[CrossRef](#)] [[PubMed](#)]
33. Tsai, S.-H.; Hsiao, Y.-C.; Chang, P.E.; Kuo, C.-E.; Lai, M.-C.; Chuang, H.-w. Exploring the biologically active metabolites produced by *Bacillus cereus* for plant growth promotion, heat stress tolerance, and resistance to bacterial soft rot in *Arabidopsis*. *Metabolites* **2023**, *13*, 676. [[CrossRef](#)]
34. Williams, A.; Langridge, H.; Straathof, A.L.; Muhamadali, H.; Hollywood, K.A.; Goodacre, R.; de Vries, F.T. Root functional traits explain root exudation rate and composition across a range of grassland species. *J. Ecol.* **2022**, *110*, 21–33. [[CrossRef](#)]
35. Kieseewalter, H.T.; Lozano-Andrade, C.N.; Wibowo, M.; Strube, M.L.; Maróti, G.; Snyder, D.; Jørgensen, T.S.; Larsen, T.O.; Cooper, V.S.; Weber, T. Genomic and chemical diversity of *Bacillus subtilis* secondary metabolites against plant pathogenic fungi. *Msystems* **2021**, *6*, e00770-20. [[CrossRef](#)] [[PubMed](#)]
36. May, J.J.; Wendrich, T.M.; Marahiel, M.A. The *dhb* operon of *Bacillus subtilis* encodes the biosynthetic template for the catecholic siderophore 2, 3-dihydroxybenzoate-glycine-threonine trimeric ester bacillibactin. *J. Biol. Chem.* **2001**, *276*, 7209–7217. [[CrossRef](#)] [[PubMed](#)]
37. Reuter, K.; Mofid, M.R.; Marahiel, M.A.; Ficner, R. Crystal structure of the surfactin synthetase-activating enzyme Sfp: A prototype of the 4'-phosphopantetheinyl transferase superfamily. *EMBO J.* **1999**, *18*, 6823–6831. [[CrossRef](#)]
38. Fira, D.; Dimkić, I.; Berić, T.; Lozo, J.; Stanković, S. Biological control of plant pathogens by *Bacillus* species. *J. Biotechnol.* **2018**, *285*, 44–55. [[CrossRef](#)]
39. Ploetz, R.C. Fusarium wilt of banana is caused by several pathogens referred to as *Fusarium oxysporum* f. sp. *cubense*. *Phytopathology* **2006**, *96*, 653–656. [[CrossRef](#)]
40. Rodríguez, H.; Fraga, R. Phosphate solubilizing bacteria and their role in plant growth promotion. *Biotechnol. Adv.* **1999**, *17*, 319–339. [[CrossRef](#)]
41. González-Cruz, J.; Pastenes, C. Water-stress-induced thermotolerance of photosynthesis in bean (*Phaseolus vulgaris* L.) plants: The possible involvement of lipid composition and xanthophyll cycle pigments. *Environ. Exp. Bot.* **2012**, *77*, 127–140. [[CrossRef](#)]
42. Cuellar-Ortiz, S.; De Lapaz Arrieta-Montiel, M.; Acosta-Gallegos, J.; Covarrubias, A.A. Relationship between carbohydrate partitioning and drought resistance in common bean. *Plant Cell Environ.* **2008**, *31*, 1399–1409. [[CrossRef](#)]
43. Saleem, M.H.; Fahad, S.; Khan, S.U.; Din, M.; Ullah, A.; Sabagh, A.E.L.; Hossain, A.; Llanes, A.; Liu, L. Copper-induced oxidative stress, initiation of antioxidants and phytoremediation potential of flax (*Linum usitatissimum* L.) seedlings grown under the mixing of two different soils of China. *Environ. Sci. Pollut. Res.* **2020**, *27*, 5211–5221. [[CrossRef](#)] [[PubMed](#)]
44. Angulo-Bejarano, P.I.; Puente-Rivera, J.; Cruz-Ortega, R. Metal and metalloid toxicity in plants: An overview on molecular aspects. *Plants* **2021**, *10*, 635. [[CrossRef](#)] [[PubMed](#)]
45. Garcin, C.; Lohmann, A.; Lamodièrre, E.; Catinot, J.; Buchala, A.; Doermann, P.; Métraux, J.-P. Characterization and biological function of the *ISOCHORISMATE SYNTHASE2* gene of *Arabidopsis*. *Plant Physiol.* **2008**, *147*, 1279–1287. [[CrossRef](#)]
46. Falk, A.; Feys, B.J.; Frost, L.N.; Jones, J.D.; Daniels, M.J.; Parker, J.E. EDS1, an essential component of R gene-mediated disease resistance in *Arabidopsis* has homology to eukaryotic lipases. *Proc. Natl. Acad. Sci. USA* **1999**, *96*, 3292–3297. [[CrossRef](#)]
47. Wang, L.; Tsuda, K.; Sato, M.; Cohen, J.D.; Katagiri, F.; Glazebrook, J. *Arabidopsis* CaM binding protein CBP60g contributes to MAMP-induced SA accumulation and is involved in disease resistance against *Pseudomonas syringae*. *PLoS Pathog.* **2009**, *5*, e1000301. [[CrossRef](#)]
48. Bell, E.; Creelman, R.A.; Mullet, J.E. A chloroplast lipooxygenase is required for wound-induced jasmonic acid accumulation in *Arabidopsis*. *Proc. Natl. Acad. Sci. USA* **1995**, *92*, 8675–8679. [[CrossRef](#)]
49. Sobajima, H.; Takeda, M.; Sugimori, M.; Kobashi, N.; Kiribuchi, K.; Cho, E.-M.; Akimoto, C.; Yamaguchi, T.; Minami, E.; Shibuya, N. Cloning and characterization of a jasmonic acid-responsive gene encoding 12-oxophytodienoic acid reductase in suspension-cultured rice cells. *Planta* **2003**, *216*, 692–698. [[CrossRef](#)]
50. Boter, M.; Ruíz-Rivero, O.; Abdeen, A.; Prat, S. Conserved MYC transcription factors play a key role in jasmonate signaling both in tomato and *Arabidopsis*. *Genes Dev.* **2004**, *18*, 1577–1591. [[CrossRef](#)]
51. Tan, B.C.; Joseph, L.M.; Deng, W.T.; Liu, L.; Li, Q.B.; Cline, K.; McCarty, D.R. Molecular characterization of the *Arabidopsis* 9-cis epoxy-carotenoid dioxygenase gene family. *Plant J.* **2003**, *35*, 44–56. [[CrossRef](#)] [[PubMed](#)]
52. Chen, W.; Wang, W.; Lyu, Y.; Wu, Y.; Huang, P.; Hu, S.; Wei, X.; Jiao, G.; Sheng, Z.; Tang, S. OsVP1 activates Sdr4 expression to control rice seed dormancy via the ABA signaling pathway. *Crop J.* **2021**, *9*, 68–78. [[CrossRef](#)]
53. Fujita, Y.; Fujita, M.; Shinozaki, K.; Yamaguchi-Shinozaki, K. ABA-mediated transcriptional regulation in response to osmotic stress in plants. *J. Plant Res.* **2011**, *24*, 509–525. [[CrossRef](#)] [[PubMed](#)]

54. Sakuma, Y.; Maruyama, K.; Qin, F.; Osakabe, Y.; Shinozaki, K.; Yamaguchi-Shinozaki, K. Dual function of an Arabidopsis transcription factor DREB2A in water-stress-responsive and heat-stress-responsive gene expression. *Proc. Natl. Acad. Sci. USA* **2006**, *103*, 18822–18827. [[CrossRef](#)]
55. Gadjev, I.; Vanderauwera, S.; Gechev, T.S.; Laloi, C.; Minkov, I.N.; Shulaev, V.; Apel, K.; Inzé, D.; Mittler, R.; Van Breusegem, F. Transcriptomic footprints disclose specificity of reactive oxygen species signaling in *Arabidopsis*. *Plant Physiol.* **2006**, *141*, 436–445. [[CrossRef](#)]
56. Davletova, S.; Schlauch, K.; Coutu, J.; Mittler, R. The zinc-finger protein Zat12 plays a central role in reactive oxygen and abiotic stress signaling in *Arabidopsis*. *Plant Physiol.* **2005**, *139*, 847–856. [[CrossRef](#)]
57. Davletova, S.; Rizhsky, L.; Liang, H.; Shengqiang, Z.; Oliver, D.J.; Coutu, J.; Shulaev, V.; Schlauch, K.; Mittler, R. Cytosolic ascorbate peroxidase 1 is a central component of the reactive oxygen gene network of *Arabidopsis*. *Plant Cell* **2005**, *17*, 268–281. [[CrossRef](#)]
58. Levine, A.; Tenhaken, R.; Dixon, R.; Lamb, C. H<sub>2</sub>O<sub>2</sub> from the oxidative burst orchestrates the plant hypersensitive disease resistance response. *Cell* **1994**, *79*, 583–593. [[CrossRef](#)] [[PubMed](#)]
59. Singh, A.; Sharma, M.K.; Sengar, R.S. Osmolytes: Proline metabolism in plants as sensors of abiotic stress. *J. Appl. Nat. Sci.* **2017**, *9*, 2079–2092. [[CrossRef](#)]
60. Andersson, J.; Wentworth, M.; Walters, R.G.; Howard, C.A.; Ruban, A.V.; Horton, P.; Jansson, S. Absence of the Lhcb1 and Lhcb2 proteins of the light-harvesting complex of photosystem II—Effects on photosynthesis, grana stacking and fitness. *Plant J.* **2003**, *35*, 350–361.
61. Asai, T.; Tena, G.; Plotnikova, J.; Willmann, M.R.; Chiu, W.L.; Gomez-Gomez, L.; Boller, T.; Ausubel, F.M.; Sheen, J. MAP kinase signalling cascade in *Arabidopsis* innate immunity. *Nature* **2002**, *415*, 977–983. [[CrossRef](#)] [[PubMed](#)]
62. Boudsocq, M.; Willmann, M.R.; McCormack, M.; Lee, H.; Shan, L.B.; He, P.; Bush, J.; Cheng, S.H.; Sheen, J. Differential innate immune signalling via Ca<sup>2+</sup> sensor protein kinases. *Nature* **2010**, *464*, 418–422. [[CrossRef](#)]
63. Cao, H.; Bowling, S.A.; Gordon, A.S.; Dong, X. Characterization of an *Arabidopsis* mutant that is nonresponsive to inducers of systemic acquired resistance. *Plant Cell* **1994**, *6*, 1583–1592. [[CrossRef](#)] [[PubMed](#)]
64. Grover, A. Plant chitinases: Genetic diversity and physiological roles. *Crit. Rev. Plant Sci.* **2012**, *31*, 57–73. [[CrossRef](#)]
65. Bohlmann, H.; Vignutelli, A.; Hilpert, B.; Miersch, O.; Wasternack, C.; Apela, K. Wounding and chemicals induce expression of the *Arabidopsis thaliana* gene Thi2.1, encoding a fungal defense thionin, via the octadecanoid pathway. *FEBS Lett.* **1998**, *437*, 281–286. [[CrossRef](#)] [[PubMed](#)]
66. Chapman, J.M.; Muhlemann, J.K.; Gayomba, S.R.; Muday, G.K. RBOH-dependent ROS synthesis and ROS scavenging by plant specialized metabolites to modulate plant development and stress responses. *Chem. Res. Toxicol.* **2019**, *32*, 370–396. [[CrossRef](#)]
67. Foreman, J.; Demidchik, V.; Bothwell, J.H.; Mylona, P.; Miedema, H.; Torres, M.A.; Linstead, P.; Costa, S.; Brownlee, C.; Jones, J.D.; et al. Reactive oxygen species produced by NADPH oxidase regulate plant cell growth. *Nature* **2003**, *422*, 442–446. [[CrossRef](#)]
68. Ma, X.; Zhang, X.; Yang, L.; Tang, M.; Wang, K.; Wang, L.; Bai, L.; Song, C. Hydrogen peroxide plays an important role in PERK4-mediated abscisic acid-regulated root growth in *Arabidopsis*. *Funct. Plant Biol.* **2019**, *46*, 165–174. [[CrossRef](#)]
69. Dennis, P.G.; Miller, A.J.; Hirsch, P.R. Are root exudates more important than other sources of rhizodeposits in structuring rhizosphere bacterial communities? *FEMS Microbiol. Ecol.* **2010**, *72*, 313–327. [[CrossRef](#)]
70. Kaspar, F.; Neubauer, P.; Gimpel, M. Bioactive secondary metabolites from *Bacillus subtilis*: A comprehensive review. *J. Nat. Prod.* **2019**, *82*, 2038–2053. [[CrossRef](#)]
71. Falardeau, J.; Wise, C.; Novitsky, L.; Avis, T.J. Ecological and mechanistic insights into the direct and indirect antimicrobial properties of *Bacillus subtilis* lipopeptides on plant pathogens. *J. Chem. Ecol.* **2013**, *39*, 869–878. [[CrossRef](#)]
72. Gayomba, S.R.; Muday, G.K. Flavonols regulate root hair development by modulating accumulation of reactive oxygen species in the root epidermis. *Development* **2020**, *147*, dev185819. [[CrossRef](#)] [[PubMed](#)]
73. Lehmann, T.; Janowitz, T.; Sánchez-Parra, B.; Alonso, M.P.; Trompeter, I.; Piotrowski, M.; Pollmann, S. *Arabidopsis* NITRILASE 1 contributes to the regulation of root growth and development through modulation of auxin biosynthesis in seedlings. *Front. Plant Sci.* **2017**, *8*, 36. [[CrossRef](#)] [[PubMed](#)]
74. Goswami, D.; Thakker, J.N.; Dhandhukia, P.C. Portraying mechanics of plant growth promoting rhizobacteria (PGPR): A review. *Cogent Food Agric.* **2016**, *2*, 1127500. [[CrossRef](#)]
75. Farag, M.A.; Zhang, H.; Ryu, C.-M. Dynamic chemical communication between plants and bacteria through airborne signals: Induced resistance by bacterial volatiles. *J. Chem. Ecol.* **2013**, *39*, 1007–1018. [[CrossRef](#)] [[PubMed](#)]
76. Ling, L.; Cheng, W.; Jiang, K.; Jiao, Z.; Luo, H.; Yang, C.; Pang, M.; Lu, L. The antifungal activity of a serine protease and the enzyme production of characteristics of *Bacillus licheniformis* TG116. *Arch. Microbiol.* **2022**, *204*, 601. [[CrossRef](#)]
77. Cheng, Z.; Li, J.-F.; Niu, Y.; Zhang, X.-C.; Woody, O.Z.; Xiong, Y.; Djonović, S.; Millet, Y.; Bush, J.; McConkey, B.J. Pathogen-secreted proteases activate a novel plant immune pathway. *Nature* **2015**, *521*, 213–216. [[CrossRef](#)]
78. Yu, X.; Ai, C.; Xin, L.; Zhou, G. The siderophore-producing bacterium, *Bacillus subtilis* CAS15, has a biocontrol effect on Fusarium wilt and promotes the growth of pepper. *Eur. J. Soil. Biol.* **2011**, *47*, 138–145. [[CrossRef](#)]
79. Nalli, Y.; Singh, S.; Gajjar, A.; Mahizhaveri, B.; Dusthacker, V.N.A.; Shinde, P.B. Bacillibactin class siderophores produced by the endophyte *Bacillus subtilis* NPROOT3 as antimycobacterial agents. *Lett. Appl. Microbiol.* **2023**, *76*, ovac026.

80. Otero, A.; Vincenzini, M. Extracellular polysaccharide synthesis by *Nostoc* strains as affected by N source and light intensity. *J. Biotechnol.* **2003**, *102*, 143–152. [[CrossRef](#)]
81. Skorupska, A.; Janczarek, M.; Marczak, M.; Mazur, A.; Król, J. Rhizobial exopolysaccharides: Genetic control and symbiotic functions. *Microb. Cell Factories* **2006**, *5*, 7. [[CrossRef](#)]
82. Naseem, H.; Bano, A. Role of plant growth-promoting rhizobacteria and their exopolysaccharide in drought tolerance of maize. *J. Plant Interact.* **2014**, *9*, 689–701. [[CrossRef](#)]
83. Naseem, H.; Ahsan, M.; Shahid, M.A.; Khan, N. Exopolysaccharides producing rhizobacteria and their role in plant growth and drought tolerance. *J. Basic Microbiol.* **2018**, *58*, 1009–1022. [[CrossRef](#)] [[PubMed](#)]
84. Kasotia, A.; Varma, A.; Tuteja, N.; Choudhary, D.K. Amelioration of soybean plant from saline-induced condition by exopolysaccharide producing *Pseudomonas*-mediated expression of high affinity K<sup>+</sup>-transporter (HKT1) gene. *Curr. Sci.* **2016**, *111*, 1961–1967. [[CrossRef](#)]
85. Thalmann, M.; Santelia, D. Starch as a determinant of plant fitness under abiotic stress. *New Phytol.* **2017**, *214*, 943–951. [[CrossRef](#)]
86. Krasensky, J.; Jonak, C. Drought, salt, and temperature stress-induced metabolic rearrangements and regulatory networks. *J. Exp. Bot.* **2012**, *63*, 1593–1608. [[CrossRef](#)] [[PubMed](#)]
87. Kaplan, F.; Guy, C.L.  $\beta$ -Amylase induction and the protective role of maltose during temperature shock. *Plant Physiol.* **2004**, *135*, 1674–1684. [[CrossRef](#)]
88. Skirycz, A.; De Bodt, S.; Obata, T.; De Clercq, I.; Claeys, H.; De Rycke, R.; Andriankaja, M.; Van Aken, O.; Van Breusegem, F.; Fernie, A.R. Developmental stage specificity and the role of mitochondrial metabolism in the response of *Arabidopsis* leaves to prolonged mild osmotic stress. *Plant Physiol.* **2010**, *152*, 226–244. [[CrossRef](#)]
89. Hoermiller, I.I.; Naegle, T.; Augustin, H.; Stutz, S.; Weckwerth, W.; Heyer, A.G. Subcellular reprogramming of metabolism during cold acclimation in *Arabidopsis thaliana*. *Plant Cell Environ.* **2017**, *40*, 602–610. [[CrossRef](#)]
90. Rezaul, I.M.; Baohua, F.; Tingting, C.; Weimeng, F.; Caixia, Z.; Longxing, T.; Guanfu, F. Abscisic acid prevents pollen abortion under high-temperature stress by mediating sugar metabolism in rice spikelets. *Physiol. Plant* **2019**, *165*, 644–663. [[CrossRef](#)]
91. Hu, Y.-F.; Li, Y.-P.; Zhang, J.; Liu, H.; Tian, M.; Huang, Y. Binding of ABI4 to a CACCG motif mediates the ABA-induced expression of the ZmSSI gene in maize (*Zea mays* L.) endosperm. *J. Exp. Bot.* **2012**, *63*, 5979–5989. [[CrossRef](#)] [[PubMed](#)]
92. Hendriks, J.H.M.; Kolbe, A.; Gibon, Y.; Stitt, M.; Geigenberger, P. ADP-glucose pyrophosphorylase is activated by posttranslational redox-modification in response to light and to sugars in leaves of *Arabidopsis* and other plant species. *Plant Physiol.* **2003**, *133*, 838–849. [[CrossRef](#)]
93. Rook, F.; Corke, F.; Card, R.; Munz, G.; Smith, C.; Bevan, M.W. Impaired sucrose-induction mutants reveal the modulation of sugar-induced starch biosynthetic gene expression by abscisic acid signalling. *Plant J.* **2001**, *26*, 421–433. [[CrossRef](#)] [[PubMed](#)]
94. Rubio, S.; Noriega, X.; Pérez, F.J. ABA promotes starch synthesis and storage metabolism in dormant grapevine buds. *J. Plant Physiol.* **2019**, *234–235*, 1–8. [[CrossRef](#)]
95. Székely, G.; Abrahám, E.; Cséplő, A.; Rigó, G.; Zsigmond, L.; Csiszár, J.; Ayaydin, F.; Strizhov, N.; Jásik, J.; Schmelzer, E.; et al. Duplicated P5CS genes of *Arabidopsis* play distinct roles in stress regulation and developmental control of proline biosynthesis. *Plant J.* **2008**, *53*, 11–28. [[CrossRef](#)] [[PubMed](#)]
96. Strizhov, N.; Abrahám, E.; Ökrész, L.; Blickling, S.; Zilberstein, A.; Schell, J.; Koncz, C.; Szabados, L. Differential expression of two P5CS genes controlling proline accumulation during salt-stress requires ABA and is regulated by ABA1, ABI1 and AXR2 in *Arabidopsis*. *Plant J.* **1997**, *12*, 557–569.
97. Altschul, S.F.; Gish, W.; Miller, W.; Myers, E.W.; Lipman, D.J. Basic local alignment search tool. *J. Mol. Biol.* **1990**, *215*, 403–410. [[CrossRef](#)]
98. Kumar, S.; Stecher, G.; Li, M.; Nnyaz, C.; Tamura, K. MEGA X: Molecular evolutionary genetics analysis across computing platforms. *Mol. Biol. Evol.* **2018**, *35*, 1547–1549. [[CrossRef](#)] [[PubMed](#)]
99. Jahn, C.E.; Charkowski, A.O.; Willis, D.K. Evaluation of isolation methods and RNA integrity for bacterial RNA quantitation. *J. Microbiol. Methods* **2008**, *7*, 318–324. [[CrossRef](#)]
100. Bankevich, A.; Nurk, S.; Antipov, D.; Gurevich, A.; Dvorkin, M.; Kulikov, A.S.; Lesin, V.; Nikolenko, S.; Pham, S.; Pribelski, A.; et al. SPAdes: A new genome assembly algorithm and its applications to single-cell sequencing. *J. Comput. Biol.* **2012**, *19*, 455–477. [[CrossRef](#)]
101. Lagesen, K.; Hallin, P.F.; Rødland, E.; Stærfeldt, H.H.; Rognes, T.; Ussery, D.W. RNAmmer: Consistent annotation of rRNA genes in genomic sequences. *Nucleic Acids Res.* **2007**, *35*, 3100–3108. [[CrossRef](#)]
102. Chan, P.P.; Lowe, T.M. tRNAscan-SE: Searching for tRNA genes in genomic sequences. In *Gene Prediction; Methods in Molecular Biology*; Springer: Berlin/Heidelberg, Germany, 2019; Volume 1962, pp. 1–14.
103. Delcher, A.L.; Harmon, D.; Kasif, S.; White, O.; Salzberg, S.L. Improved microbial gene identification with GLIMMER. *Nucleic Acids Res.* **1999**, *27*, 4636–4641. [[CrossRef](#)]
104. Tatusov, R.L.; Fedorova, N.D.; Jackson, J.D.; Jacobs, A.R.; Kiryutin, B.; Koonin, E.V.; Krylov, D.M.; Mazumder, R.; Mekhedov, S.L.; Nikolskaya, A.N.; et al. The COG database: An updated version includes eukaryotes. *BMC Bioinform.* **2003**, *4*, 41. [[CrossRef](#)] [[PubMed](#)]
105. Moriya, Y.; Itoh, M.; Okuda, S.; Yoshizawa, A.; Kanehisa, M. KAAAS: An automatic genome annotation and pathway reconstruction server. *Nucleic Acids Res.* **2007**, *35*, W182–W185. [[CrossRef](#)]

106. Chen, T.W.; Gan, R.C.R.; Wu, T.H.; Huang, P.J.; Lee, C.Y.; Chen, Y.Y.M.; Chen, C.C.; Tang, P. FastAnnotator: An efficient transcript annotation web tool. *BMC Genom.* **2012**, *13* (Suppl. S7), S9. [[CrossRef](#)]
107. Alcock, B.P.; Raphenya, A.R.; Lau, T.T.Y.; Tsang, K.K.; Bouchard, M.; Edalatmand, A.; Huynh, W.; Nguyen, A.V.; Cheng, A.A.; Liu, S.; et al. CARD 2020: Antibiotic resistance surveillance with the comprehensive antibiotic resistance database. *Nucleic Acids Res.* **2020**, *48*, D517–D525. [[CrossRef](#)]
108. Nwosu, I.G.; Abu, G.O.; Agwa, K.O. Isolation, screening and characterization of exopolysaccharide producing bacteria. *Microbiol. Res. J. Int.* **2019**, *29*, 1–9. [[CrossRef](#)]
109. Govender, N.T.; Mahmood, M.; Seman, I.A.; Wong, M.-Y. The phenylpropanoid pathway and lignin in defense against *Ganoderma boninense* colonized root tissues in oil palm (*Elaeis guineensis* Jacq.). *Front. Plant Sci.* **2017**, *8*, 1395. [[CrossRef](#)]
110. Bruce, R.J.; West, C.A. Elicitation of lignin biosynthesis and isoperoxidase activity by pectic fragments in suspension cultures of castor bean. *Plant Physiol.* **1989**, *91*, 889–897. [[CrossRef](#)] [[PubMed](#)]
111. DeLong, J.M.; Prange, R.K.; Hodges, D.M.; Forney, C.F.; Bishop, M.C.; Quilliam, M. Using a modified ferrous oxidation–xylenol orange (FOX) assay for detection of lipid hydroperoxides in plant tissue. *J. Agric. Food Chem.* **2002**, *50*, 248–254. [[CrossRef](#)]
112. Nakano, Y.; Asada, K. Hydrogen peroxide is scavenged by ascorbate-specific peroxidase in spinach chloroplasts. *Plant Cell Physiol.* **1981**, *22*, 867–880.
113. Aebi, H. Catalase in vitro. *Methods Enzymol.* **1984**, *105*, 121–126. [[PubMed](#)]
114. Tsai, H.-L.; Lue, W.-L.; Lu, K.-J.; Hsieh, M.-H.; Wang, S.-M.; Chen, J. Starch synthesis in *Arabidopsis* is achieved by spatial cotranscription of core starch metabolism genes. *Plant Physiol.* **2009**, *151*, 1582–1595. [[CrossRef](#)]
115. Kurniawan, A.; Chuang, H.W. Rhizobacterial *Bacillus mycoides* functions in stimulating the antioxidant defence system and multiple phytohormone signalling pathways to regulate plant growth and stress tolerance. *J. Appl. Microbiol.* **2022**, *132*, 1260–1274. [[CrossRef](#)] [[PubMed](#)]
116. Lee Downing, W.; Mauxion, F.; Fauvaque, M.-O.; Reviron, M.-P.; de Vienne, D.; Vartanian, N.; Giraudat, J. A *Brassica napus* transcript encoding a protein related to the Kunitz protease inhibitor family accumulates upon water stress in leaves, not in seeds. *Plant J.* **1992**, *2*, 685–693. [[CrossRef](#)]

**Disclaimer/Publisher’s Note:** The statements, opinions and data contained in all publications are solely those of the individual author(s) and contributor(s) and not of MDPI and/or the editor(s). MDPI and/or the editor(s) disclaim responsibility for any injury to people or property resulting from any ideas, methods, instructions or products referred to in the content.